

1 **Improving soil carbon estimates by linking conceptual pools against measurable carbon**
2 **fractions in the DAYCENT Model Version 4.5**

3
4 Shree R.S. Dangal^{1,*}, Christopher Schwalm¹, Michel A. Cavigelli², Hero T. Gollany³, Virginia
5 L. Jin⁴ & Jonathan Sanderman¹

6 ¹Woodwell Climate Research Center, 149 Woods Hole Road, Falmouth, MA 02540, USA

7 ²US Department of Agriculture - Agricultural Research Service, Sustainable Agricultural
8 Systems Laboratory, Beltsville Agricultural Research Center, Beltsville, MD 20705, USA

9 ³US Department of Agriculture - Agriculture Research Service, Columbia Plateau Conservation
10 Research Center, Pendleton, OR 97810, USA

11 ⁴US Department of Agriculture - Agricultural Research Service, Agroecosystem Management
12 Research Unit, University of Nebraska-Lincoln, NE 68583, USA

13
14 *Correspondence to:* Shree R.S. Dangal (shree.dangal@unl.edu)

15 **Current Address:* School of Natural Resources, University of Nebraska-Lincoln, NE 68583

16
17
18
19 **Key points:**

- 20 1. The modified model overestimated measured SOC values at long term research sites but
21 better approximated derived SOC values from other data products when calibrated to
22 carbon (C) fraction compared to the default model.
23 2. Model modifications led to larger absolute and relative losses of SOC compared to the
24 default model during 1895-2005.
25 3. Under the RCP8.5 scenario, projected SOC losses with the modified model were 33%
26 and 29% larger for croplands and grasslands, respectively, compared to the default
27 model.

28 **Abstract**

29 Terrestrial soil organic carbon (SOC) dynamics play an important but uncertain role in the global
30 carbon (C) cycle. Current modeling efforts to quantify SOC dynamics in response to global
31 environmental changes do not accurately represent the size, distribution and flux of C from the
32 soil. Here, we modified the Daily Century (DAYCENT) biogeochemical model by parameterizing
33 conceptual SOC pools with C fraction data, followed by historical and future simulations of SOC
34 dynamics. Results showed that simulations using modified DAYCENT (DC_{mod}) led to better
35 initialization of SOC stocks and distribution compared to default DAYCENT (DC_{def}) at long-term
36 research sites. Regional simulation using DC_{mod} demonstrated higher SOC stocks for both
37 croplands (34.86 vs 26.17 $MgC\ ha^{-1}$) and grasslands (54.05 vs 40.82 $MgC\ ha^{-1}$) compared to DC_{def}
38 for the contemporary period (2001-2005 average), which better matched observationally
39 constrained data-driven maps of current SOC distributions. Projection of SOC dynamics to land
40 cover change (IPCC AR4 A2 scenario) under IPCC AR5 RCP8.5 climate scenario showed
41 absolute SOC loss of 8.44 and 10.43 $MgC\ ha^{-1}$ for grasslands and croplands, respectively, using
42 DC_{mod} whereas, SOC losses were 6.55 and 7.85 $MgC\ ha^{-1}$ for grasslands and croplands,
43 respectively, using DC_{def} . The projected SOC loss using DC_{mod} was 33% and 29% higher for
44 croplands and grasslands compared to DC_{def} . Our modeling study demonstrates that initializing
45 SOC pools with C fraction data led to more accurate representation of SOC stocks and individual
46 carbon pool, resulting in larger absolute and relative SOC losses due to agricultural intensification
47 in the warming climate.

48

49 **1. Introduction**

50 Soil is the largest terrestrial reservoir of organic carbon (C), storing about 1500 Pg C in the top
51 100 cm (Batjes, 2016; Nachtergaele et al., 2012). Any small changes in the magnitude, distribution
52 and forms of terrestrial soil organic carbon (SOC) may lead to large release of C to the atmosphere
53 (Sulman et al., 2018), with significant impact on food security and the global climate system (Lal,
54 2004). Given that changes in SOC represent one of the largest uncertainties in the global C budget
55 (Ciais et al., 2014), accurate quantification of the distribution and forms of SOC can help to
56 constrain the global C budget and provide key insights on the underlying processes related to SOC
57 protection and cycling (Stockmann et al., 2013).

58 Changes in SOC stocks at any given time depend on the balance between organic matter inputs
59 via plant production, additions of manure and compost, and outputs via decomposition, erosion
60 and hydrologic leaching of various C compounds (Davidson and Janssens, 2006; Jobbágy and
61 Jackson, 2000). Although higher organic matter inputs to the soil generally correlate with high
62 SOC (Sanderman et al., 2017a), the biological stability of SOC is ultimately determined by the
63 interactions among the soil physicochemical environment (soil moisture, temperature, pH and
64 aeration), soil mineralogy, and the accessibility of the organic matter to microbes and enzymes
65 (Schmidt et al., 2011). Current understanding of the SOC dynamics indicates that the soil
66 physicochemical environment plays an important role in determining the C efflux from soil and
67 that the efflux rates are modified by substrate availability and the affinities of enzymes for the
68 substrates (Six et al., 2002). However, the extent to which different physicochemical
69 characteristics of soil control the stabilization and cycling of SOC is still debated (Carvalhais et
70 al., 2014; Doetterl et al., 2015; Rasmussen et al., 2018). Additionally, the complex molecular
71 structure of C substrates and their sensitivity to climatic and environmental constraints add further

72 complexity in understanding SOC dynamics at different spatial and temporal scales (Davidson and
73 Janssens, 2006).

74 Previous studies have shown that the factors affecting the stabilization/destabilization of SOC are
75 numerous and that the changes in SOC over space and time are the result of complex interactions
76 among climatic, biotic and edaphic factors (Rasmussen et al., 2018; Stockmann et al., 2013; Torn
77 et al., 1997; Wiesmeier et al., 2019). For example, Carvalhais et al. (2014) have shown that climate,
78 particularly temperature, strongly controls SOC turnover. Doetterl et al. (2015) found that
79 geochemical characteristics such as base saturation, soil texture, silica content and pH also play a
80 dominant role by altering the adsorption and aggregation of SOC. In addition, other studies
81 indicate that soil nitrogen (N) availability affects SOC change due to constraints on microbial
82 activity and plant productivity (Grandy et al., 2008; Janssens et al., 2010; Sinsabaugh et al., 2005).
83 These findings have led to the view that the accumulation and decomposition of organic matter in
84 soil is ultimately determined by the interactions among climate, vegetation type, topography and
85 lithology.

86 Biogeochemical models commonly rely on capturing SOC heterogeneity associated with the
87 complex interactions among climatic, biotic and edaphic factors by defining a number of distinct
88 SOC pools with different potential turnover rates (Tian et al., 2015; Todd-Brown et al., 2014). The
89 potential turnover rates of distinct soil pools are modified by climatic factors such as soil moisture
90 and temperature, soil chemical factors such as pH and oxygen availability and the mechanism that
91 facilitates C protection via organo-mineral interactions and aggregation, often loosely represented
92 by clay content (Trumbore, 1997). Each of these pools is conceptual in nature, implying that the
93 turnover times of these pools cannot be determined by chemical and physical fractionation (Paul

94 et al., 2001). As a result, there is increasing need and effort to link the conceptual pools with some
95 measurable data to determine the turnover rates of SOC pools in the biogeochemical models.

96 In current biogeochemical models, there is a general agreement that the soil organic matter (SOM)
97 contains at least three C pools: an active pool dominated by root exudates and the rapidly
98 decomposable components of fresh plant litter, with mean residence time (MRT) ranging from
99 days to years (Hsieh, 1993); a slow pool dominated by decomposed organic material, often of
100 microbial origin, with MRT ranging from years to centuries (Torn et al., 2013); and a passive pool
101 dominated by stabilized organic matter with MRT of several hundred to thousands of years
102 (Czimczik and Masiello, 2007). Changes in the size and relative abundance of these pools are
103 strongly influenced by climate, soil type and land use (Sanderman et al., 2021). Therefore,
104 accounting for accurate distribution of SOC into different pools is paramount to quantify the
105 current SOC stocks and examine the vulnerability of SOC to future environmental changes.

106 Relating these conceptual pools with SOC partitioned into laboratory defined fractions, such as
107 particulate-, mineral associated- and pyrogenic-forms of C (POC, MOAC and PyC, respectively),
108 can help to constrain the turnover rate of different pools in biogeochemical models. For example,
109 Skjemstad et al. (2004) related POC, MOAC and PyC approximated using a combination of
110 physical size fractionation and solid-state ^{13}C -NMR spectroscopy with resistant plant material
111 (RPM), humic (HUM) and inert organic material (IOM) pools in the Rothamsted carbon (RothC)
112 model to predict changes in SOC in response to changes in soil type, climate and management.
113 However, RothC does not explicitly simulate plant growth and plant response to dynamic changes
114 in climate and other environmental factors (Zimmermann et al., 2007). In addition, the plant
115 material is loosely partitioned into decomposable and resistant forms with large uncertainties in
116 their respective sizes (Cagnarini et al., 2019). Unlike RothC, ecosystem models such as

117 Century, DeNitrification-DeComposition (DNDC) and Agricultural Production Systems
118 sIMulator (APSIM) integrate the effects of climate, land use change and land management
119 practices by simulating plant physiology and soil biogeochemistry, and explicitly consider the
120 effects of climate, land use and land management on three conceptual soil C pools with different
121 turnover rates (Hartman et al., 2011; Ogle et al., 2010).

122 In this study, we modified, calibrated and evaluated the version 4.5 of the Daily Century model
123 (hereafter, DAYCENT) to improve the representation of SOC dynamics by linking conceptual
124 pools of active, slow and passive SOC against estimates of the measurable POC, MOAC and PyC
125 fractions, respectively. We then simulated the response of SOC to climate and land use change
126 during the historical and future period using the default (hereafter, DC_{def}) and modified (hereafter,
127 DC_{mod}) DAYCENT model in the US Great Plains ecoregion. The objectives of this study were to
128 1) modify the DC_{def} model to link active, slow and passive pools of organic C to soil C fractions;
129 2) calibrate and evaluate DC_{mod} performance by comparing the distribution of C in active, slow
130 and passive pools against C fractions predicted at seven long-term research sites; 3) evaluate the
131 differences between the DC_{mod} and DC_{def} in simulating contemporary SOC stocks and their
132 distribution by comparing against other existing data products in the US Great Plains region; and
133 4) project the SOC change in response to climate and land cover change through 2100. We
134 hypothesize that (i) calibrating the conceptual pools to C fraction data in the DAYCENT model
135 leads to more accurate initialization of equilibrium pool structure (Skjemstad et al., 2004), thereby
136 allowing a better comparison of measured and simulated SOC in response to climate, land use and
137 management (Basso et al., 2011); (ii) conversion of native vegetation to any agricultural use
138 significantly alters the distribution of SOC among the various soil pools (Guo and Gifford, 2002),
139 but the rate and extent of SOC change depend on the intensity of agricultural use (Lal, 2018; Page

140 et al., 2014), with larger losses from models that allocate more C to active and slow pools; and (iii)
141 land use under a warming climate would result in larger absolute and relative losses of SOC from
142 the model that derive more SOC from the active pool due to rapid decomposition of fresh organic
143 matter induced by warming (Crowther et al., 2016).

144 **2. Materials and methods**

145 **2.1 The DAYCENT Model**

146 The DAYCENT Version 4.5 is a daily time step version of the Century biogeochemical model that
147 simulates the dynamics of C and N of both managed and natural ecosystems (Del Grosso et al.,
148 2002; Parton et al., 1998). The exchange of C and N among the atmosphere, vegetation and soil is
149 a function of climate, land use, land management and other environmental factors. The vegetation
150 pool simulates potential plant growth at a weekly time step limited by water, light and nutrients.
151 The DAYCENT model consists of multiple pools of SOM and simulates turnover as a function of
152 the amount and quality of residue returned to the soil, the size of different soil pools and a series
153 of environmental limitations. The type and timing of management events including tillage,
154 fertilization, irrigation, harvest and grazing activities can affect plant production and SOM
155 retention.

156 The DAYCENT model was originally developed from the monthly CENTURY model version 4.0.
157 The CENTURY 4.0 is a general FORTRAN model of the plant-soil ecosystem that simulates
158 carbon and nutrient dynamics of different types of terrestrial ecosystems (grasslands, forest, crops
159 and savannas). CENTURY 4.0 primarily focused on simulation of soil organic matter dynamics
160 of agro-ecosystems (Metherell et al., 1994). Earlier development of the CENTURY focused on
161 simulation of soil organic matter dynamics of grasslands, forest and savanna ecosystems (Parton
162 et al., 1988; Sanford Jr et al., 1991).

163 The first DAYCENT model was developed in FORTRAN 77 and C from CENTURY 4.0 to
164 simulate the exchanges of C, water, nutrients, and gases (CO₂, CH₄, N₂O, NO_x, N₂) among the
165 atmosphere, soil and plants at a daily time step (Del Grosso et al., 2001; Kelly et al., 2000; Parton
166 et al., 1988). The submodels used in DAYCENT are described in detail by Del Grosso et al. (2001),
167 which includes submodels for plant productivity, soil organic matter decomposition, soil water
168 and temperature dynamics, and trace gas fluxes. Other model developments while transitioning
169 from CENTURY 4.0 to DAYCENT included dynamic carbon allocation and changes in growing
170 degree days routine that triggers the start and end of growing season based on phenology (soil
171 surface temperature, air temperature, and thermal units).

172 The first formal version DAYCENT 4.5 (Hartman et al., 2011) was developed from Del Grosso et
173 al. (2002), with a focus on simulation of trace gas fluxes for major crop types in the US Great
174 Plains region. Hartman et al. (2011) focused on calibrating and validating crop yield and trace gas
175 fluxes for all the major crop types in 21 representative counties in the US Great Plains region.

176 The SOM sub-model consists of active, slow and passive pools with different turnover times. The
177 active pool has a short (1-5 yr) turnover time and consists of live microbes and microbial products.
178 The slow pool has an intermediate turn over time (20-50 yr) and contains physically protected
179 organic matter and stabilized microbial products. The passive pool has a long turnover time (400-
180 2000 yr) with physically and chemically stabilized SOC. In DAYCENT, the turnover of the active,
181 slow and passive pools are simulated as a function of potential decomposition rates of respective
182 pools modified by soil temperature, moisture, clay content, pH and cultivation effects. Changes in
183 SOC are simulated for the top 20 cm of the soil.

184 In this study, we modified the DAYCENT and developed a methodology to calibrate the size of
185 the conceptual soil pools by comparing it with carbon fraction data at long term research sites.

186 First, we developed measurable carbon fraction data using a combination of diffuse reflectance
187 spectroscopy and a machine learning model (section 2.2). Second, we modified the DAYCENT
188 model to link conceptual active, slow, and passive pools with the carbon fraction data (section 2.3
189 & 2.4). Third, we parameterized the DAYCENT by tuning the potential decomposition rates (k)
190 such that the size of the active, slow and passive soil pools match with the POC, MAOC and PyC,
191 respectively at the long-term research sites (section 2.5). Fourth, we calibrated both the default and
192 modified DAYCENT using input data developed in section 2.3 against observed total SOC at the
193 long-term research sites (section 2.6), followed by model validation (section 2.7) and historical
194 and future simulations (section 2.8).

195 **2.2 Development of carbon fraction datasets to match with soil carbon pools**

196
197 To link the SOC pools in DAYCENT with measurable C fractions, we used seven long-term
198 research sites located in the United States (Cavigelli et al., 2008; Gollany, 2016; Ingram et al.,
199 2008; Liebig et al., 2010; Schmer et al., 2014; Sindelar et al., 2015; Syswerda et al., 2011), which
200 span a range of climatic, land use and land management gradients (Table 1). Six of seven research
201 sites are part of Long-Term Agroecosystem Research (LTAR) network focused on sustainable
202 intensification of agricultural production. The remaining site is part of Columbia Plateau
203 Conservation Research Center (CPCRC) Long-Term Experiment (LTE). At each site, we predicted
204 the POC, MAOC and PyC fractions using a diffuse reflectance mid-infrared (MIR) spectroscopy-
205 based model as detailed in Sanderman et al. (2021). The predictive models for the C fractions were
206 developed from a database of fully fractionated soil samples using a combination of physical size
207 separation and solid-state ^{13}C NMR spectroscopy (Baldock et al., 2013b) of Australian (Baldock
208 et al., 2013a) and US origin (Sanderman et al., 2021). All samples for model development were
209 scanned using a Thermo Nicolet 6700 FTIR spectrometer with Pike AutoDiff reflectance

210 accessory located at the Commonwealth Scientific and Industrial Research Organization (CSIRO)
211 in Australia. The soil samples from all the long-term research sites were scanned using a Bruker
212 Vertex 70 FTIR equipped with a Pike AutoDiff reflectance accessory located at Woodwell Climate
213 Research Center in the United States. For all samples, spectra were acquired on dried and finely
214 milled soil samples. Since the SOC fraction model and the soil samples were scanned using
215 different instruments, we developed a calibration transfer routine to account for the differences in
216 spectral responses between the CSIRO (primary) and Woodwell (secondary) instruments by
217 scanning a common set of 285 soil samples. The calibration transfer routine was developed using
218 piecewise direct standardization (PDS) as described in Dangal & Sanderman (2020).
219

220

221

Table 1. General attributes of the LTER, LTER and CPCRC-LTE sites used for DAYCENT parameterization and calibration

Site Name	Sampling Location	Lon	Lat	T _{avg} (°C)	Annual Precip. (mm)	Elev (m)	Land use	Data Avail.	Reference
Lower Ches. Bay	Beltsville, MD	-76.9	39.1	12.8	1110	41	CS	1996-2016	Cavigelli et al. 2008
CPCRC-NTLTE	Pendleton, OR	-118.4	45.4	10.6	437	456	WW-FA	2005-2014	Gollany 2016
Cent. Plains Exp. Ran.	Cheyenne, WY	-104.9	41.2	8.6	425	1930	C3-C4 Gra.	2004-2013	Ingram et al. 2008
Northern Plains	Mandan, ND	-100.9	46.8	4	416	593	C3-C4 Gra.	1959-2014	Liebig et al 2010
Platte/High Plains Aq.	Lincoln, NE	-96.5	40.9	11	728	369	CC,CS	1998-2011	Sindelar et al 2015
Platte/High Plains Aq.	Mead, NE	-96.0	41.0	9.8	740	349	CC	2001-2015	Schmer et al. 2014
Kellogg Bio. Station	H. Corners, MI	-85.4	42.4	9.7	920	288	CSW-Gra.	1989-2017	Syswerda et al. 2011 [†]

CS: Corn-Soya; WW: Winter Wheat; FA: Fallow; CC: Continuous Corn, SC: Soya-Corn, CSW: Corn-Soya-Wheat, Gra.: Grass #H. Corners, MI is a LTER & LTER site; CPCRC-NTLTE: Columbia Plateau Conservation Research Center No-Till Long-Term Experiment.

222 For estimating C fractions of the prediction set (i.e., soil spectra of seven long-term research sites),
223 we used a local memory based learning (MBL) approach that fits a unique target function
224 corresponding to each sample in the prediction set (Dangal et al., 2019; Ramirez-Lopez et al.,
225 2013). The MBL selects spectrally similar neighbors for each sample in the prediction sets to build
226 a unique SOC fraction model for each target sample. The spectrally similar neighbors were
227 optimized by developing a soil C fraction model using a range of spectrally similar neighbors and
228 selecting the neighbors that produce the minimum root mean square error based on local cross
229 validation. Before developing the soil C fraction model, the spectra of both the calibration and
230 prediction sets were baseline transformed. Following baseline transformation, spectral outliers
231 were detected using F-ratios (Hicks et al., 2015). The F-ratio estimates the probability distribution
232 function of the spectra and picks samples that fall outside the calibration space as outliers (Dangal
233 et al., 2019). Observation data used for building the soil C fraction model were square root
234 transformed before model development and later back-transformed when estimating the goodness-
235 of-fit. The performance of predictive models is shown in Table S1.

236 The predicted soil C fractions for the seven long-term research sites were then converted into C
237 fraction stocks using the relationship between C fraction (%), bulk density (BD; g/cm^3) and the
238 depth (cm) of soil samples. Since the BD data were not available for all long-term research sites
239 for different crop rotation and grazing intensities, we predicted BD using methods similar to those
240 described above. The only difference was that the samples used to develop the BD model were
241 based on a much larger database of soil spectra scanned at the Kellogg Soil Survey Laboratory
242 (KSSL) in Lincoln, USA (Dangal et al., 2019). Before predicting BD, the calibration transfer, as
243 documented in Dangal & Sanderman (2020), between the KSSL and Woodwell soil spectra were
244 developed and the local modeling approach (i.e., MBL) was used to make final prediction for

245 samples with missing laboratory BD. Calibration transfer between the spectrometers at the
246 Woodwell (secondary instrument) and KSSL (primary instrument) laboratory was necessary to
247 improve prediction of BD ($R^2 = 0.46-0.64$ and $RMSE = 0.26-0.50$) (Dangal and Sanderman, 2020).
248 One of the technical challenges associated with the comparison of simulated pool sizes against
249 diffuse reflectance spectroscopy-based predictions of POC, MOAC and PyC at long-term research
250 sites was the absence of laboratory data on C fractions to validate the MIR based predictions. To
251 address this shortcoming, we first compared the sum of the MIR based predictions of POC, MOAC
252 and PyC against observation of total SOC available at these sites (Figure S1). When comparing
253 the total SOC against MIR based predictions, we did not limit the comparison to 20 cm, but
254 allowed it across the full soil depth profile based on the availability of SOC data at the seven long-
255 term research sites. Additionally, the laboratory data used for model comparison were available at
256 multiple depths of up to 60 cm often without a direct measurement for the 0-20 cm depth
257 necessitating an approximation of the 0-20 cm stock. For example, when soils were collected from
258 0-15 and 15-30 cm, we estimated the 20 cm SOC stock by adding 1/3 of the 15-30 cm SOC stock
259 to the entire 0-15 cm SOC stock.

260 **2.3 Input datasets for driving the DAYCENT model**

261 The US Great Plains region was delineated using the Level I ecoregions map (Omernik and
262 Griffith, 2014) available through the Environmental Protection Agency (<https://www.epa.gov/ecoresearch/ecoregions-north-america>). The datasets for driving the DAYCENT were divided into
263 two parts: 1) dynamic datasets that include time series of daily climate (precipitation, maximum
264 and minimum temperature), annual land cover land use change (LCLUC) and land management
265 practices (irrigation, fertilization and cropping system, tillage intensity) and 2) static datasets that
266 include information on soil properties (soil texture, pH and bulk density) (Sanderman et al., 2021),
267

268 and topography maps (Jarvis et al., 2008). For the historical period (1895-2005), we used a
 269 combination of VEMAP and PRISM (1895-1979) and Daymet (1980-2005) (Daly and Bryant,
 270 2013; Kittel et al., 2004; Thornton et al., 2012). The VEMAP datasets are available at a daily time
 271 step and a coarser spatial resolution ($0.5^\circ \times 0.5^\circ$), while the PRISM datasets are available at a
 272 monthly time step and a finer spatial resolution ($10 \text{ km} \times 10 \text{ km}$). We interpolated the PRISM data
 273 at a daily time step by using the daily trend from the VEMAP datasets such that the monthly
 274 precipitation totals and monthly average temperature matches the monthly climate from the
 275 PRISM data. For the future (2006-2100), we used the Intergovernmental Panel on Climate Change
 276 (IPCC) 5th assessment report (AR5) RCP4.5 and RCP8.5 climate scenarios available at a spatial
 277 resolution of $1/16^\circ \times 1/16^\circ$.

278 **Table 2.** Default and modified decomposition (k) parameters used in the DAYCENT to simulate
 279 the size of different carbon pools

Pools	Default		Modified k (yr^{-1})			
	k (yr^{-1})	grid search	N	Optimized	Absolute	Relative (%)
Active	7.30	(3,12)	301	3.50	-3.80	-52
Slow	0.20	(0.10,0.30)	201	0.14	-0.06	-30
Passive	0.0045	(0.001,0.0085)	351	0.0075	0.003	+67

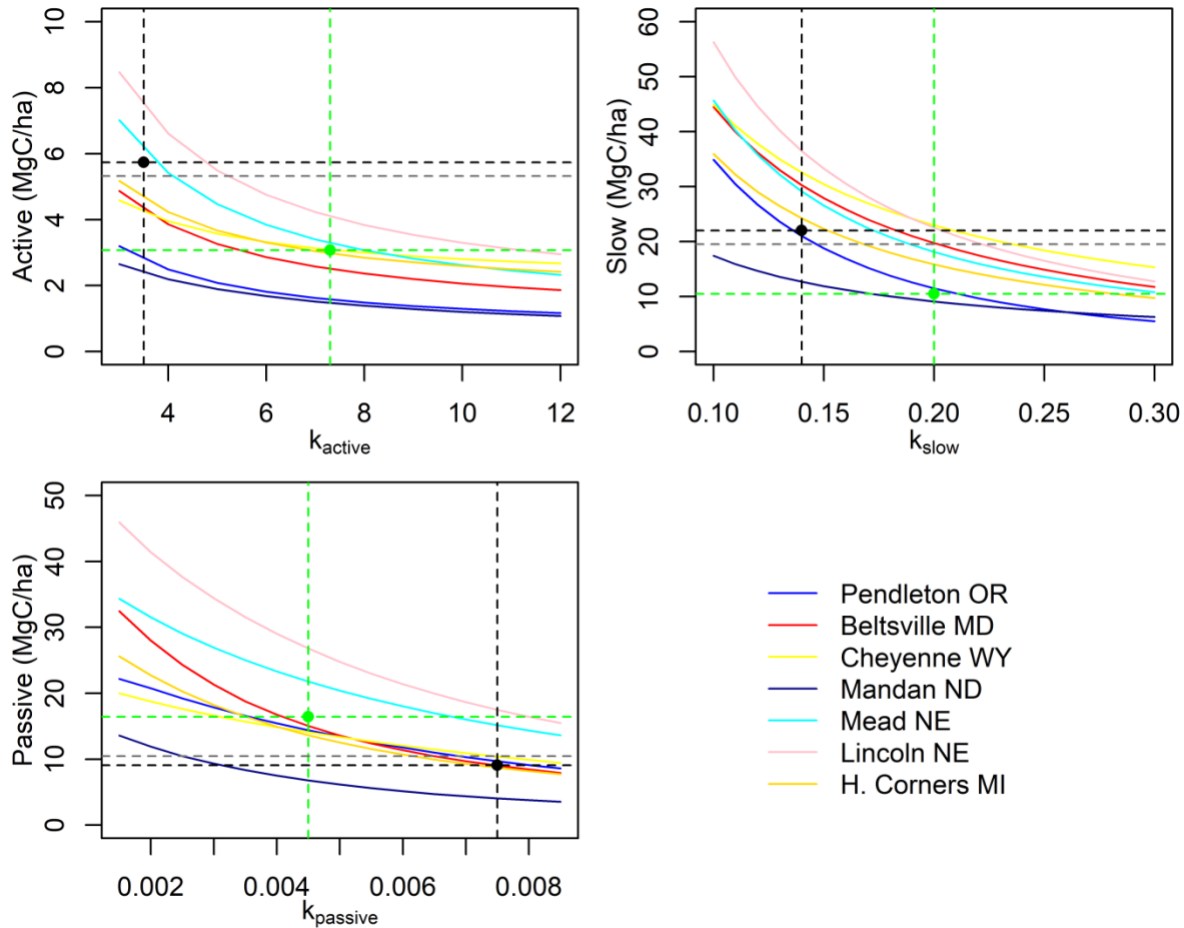
280
 281 For annual LCLUC, we used spatially explicit datasets available at a resolution of $250\text{m} \times 250\text{m}$
 282 for the historical (1938-2005) and future (2006-2100) periods under the IPCC 4th assessment report
 283 (AR4) A2 scenario (Sohl et al., 2012). We used only the A2 land cover scenario because there was
 284 not much difference in the trajectories of land cover change through 2100. For the period 1895-
 285 1937, we backcasted the proportional distribution of croplands and grasslands by integrating the
 286 Sohl et al. (2012) data with HYDE v3.2 data (Klein Goldewijk et al., 2017). We estimated the

287 fractional distribution of croplands and grasslands by calculating the total number of pixels
288 dominated by each land cover type at 250m resolution within each $1/16^\circ$ grid cell (Figure S2a).
289 Irrigation and fertilization data are based on census of agriculture statistics (Falcone and LaMotte,
290 2016). All datasets were interpolated/aggregated to a common resolution of $1/16^\circ \times 1/16^\circ$
291 (approximately 7km x 7km at the equator).
292 Cropping systems and crop rotation are based on county level data for the US Great Plains region
293 available through Hartman et al. (2011), which were merged with tillage type and intensity data
294 (Baker, 2011) to write 24 unique schedule files that describe grid-specific cropping system and
295 crop management practices. The 24 unique schedule files include sequences of time blocks, with
296 each block describing a unique set of crop types, crop rotation, tillage type, tillage intensity,
297 fertilization, irrigation and residue removal (Hartman et al., 2011). Using these schedule files, we
298 developed an unsupervised classification algorithm (K-means) to create 24 unique clusters as a
299 function of long-term average climate (precipitation, minimum- and maximum-temperatures),
300 land forms, land cover type and elevation. We then assigned all the grid cells to one of the 24
301 unique clusters to create a spatially explicit dataset on cropping system and crop rotation. While
302 developing the unsupervised classification algorithm, the eastern part of the US Great Plains region
303 dominated by corn (*Zea mays* L.) - soybean (*Glycine max* (L.) Merr.) rotation was
304 underrepresented. To address this shortcoming, we used randomly selected grid points from the
305 CropScape data (<https://nassgeodata.gmu.edu/CropScape/>) available through the USDA National
306 Agricultural Statistics Service in the unsupervised classification algorithm. Additionally, cropping
307 systems classified using the unsupervised algorithm was verified against current CropScape data
308 allowing for realistic representation of cropping systems. The distribution of schedule files
309 representing different crop rotation and crop types used to build the unsupervised classification is

310 shown in Figure S2b and the spatial distribution of crop rotations based on the unsupervised
311 classification is shown in Figure S3.

312 **2.4 Linking DAYCENT conceptual pools with C fractions**

313 The SOC dynamics in the DAYCENT consists of the first-order kinetic exchanges among
314 conceptual pools (active, slow, and passive) defined by empirical turnover rates (Parton et al.,
315 1987). However, a major impetus for quantifying these pools comes from the fact that the size and
316 distribution of SOC in the different pools cannot be directly linked with experimental data. Here,
317 we developed a methodology to link the conceptual active, slow and passive pools to spectroscopy-
318 based estimates of POC, MAOC and PyC fractions. The rate of decomposition across POC,
319 MAOC and PyC are consistent with the potential turnover rates assigned to the active, slow, and
320 passive pools in soil C models (Baldock et al., 2013b). As a result, we modified the potential
321 turnover rates in the DAYCENT model such that the absolute difference between the simulated
322 SOC and predicted C fractions was minimized (see section 2.5 below). When matching the soil
323 pools with C fraction data, we compared the sum of belowground structural, metabolic and active
324 pool SOC to POC, slow pool SOC to MAOC, and passive pool SOC to PyC. Details on matching
325 the conceptual pools with C fraction data are provided in Figure S4.



326

327 **Figure 1.** Parameterization of k_{active} , k_{slow} and $k_{passive}$ using carbon fractions predicted across long
 328 term research sites. The dashed black line represents the potential decomposition rates (k) that is
 329 optimized when the absolute difference between the DC_{mod} simulated SOC in different pools and
 330 the predicted C fractions is minimum. The dashed green line represents the size of different soil
 331 SOC pools using the default k value based on DC_{def} model. The dashed grey line is the average
 332 POC (i.e. active), MAOC (i.e. slow) and PyC (i.e. passive) predicted using the combination of
 333 diffuse reflectance spectroscopy and machine learning at seven long term research sites {Citation}.

334 2.5 Model parameterization

335 In this study, we performed a grid search to parameterize the potential decomposition rates for
 336 respective soil pools by running the DAYCENT at seven long-term research sites (Figure 1; Table

337 2), and compare the simulated SOC in active, slow, and passive pools with the POC, MAOC and
 338 PyC fractions. In the current DAYCENT model, total SOC is defined as follows:

$$339 \quad SOC_{total} = SOC_{strc} + SOC_{metab} + SOC_{active} + SOC_{slow} + SOC_{passive} \quad (1)$$

340 Where,

341 SOC_{strc} = structural SOC pool

342 SOC_{metab} = metabolic SOC pool

343 SOC_{active} = active SOC pool

344 SOC_{slow} = slow SOC pool

345 $SOC_{passive}$ = passive SOC pool

346 Each of the above SOC pool has a specific potential decomposition rates that determines the time
 347 (ranging from years to centuries) until decomposition. Plant material is transferred to the active,
 348 slow and passive pools from aboveground and belowground litter pools and three dead pools. Total
 349 C flow (CF_{act}) out of the active pool is a function of potential decomposition rates modified by the
 350 effect of moisture, temperature, pH, and soil texture.

$$351 \quad CF_{act} = k_{act} \times SOC_{act} \times bg_{dec} \times clt_{act} \times text_{ef} \times anerb_{dec} \times pH_{eff} \times dtm \quad (2)$$

352 Where,

353 CF_{act} = the total amount of C flow out of the active pool (g C m⁻²)

354 k_{act} = intrinsic decomposition rate of the active pool (yr⁻¹)

355 SOC_{act} = SOC in the active pool (g C m⁻²).

356 bg_{dec} = the effect of moisture and temperature on the decomposition rate (0-1)

357 clt_{act} = the effect of cultivation on the decomposition rate for crops (0-1) for the active pool

358 $text_{ef}$ = the effect of soil texture on the decomposition rate (0-1)

359 $anerb_{dec}$ = the effect of anaerobic conditions on the decomposition rate (0-1)

360 pH_{eff} = the effect of pH on the decomposition rate (0-1)

361 dtm = the time step (fraction of year)

362 The respiratory loss when the active pool decomposes is calculated as:

$$363 \quad CO_{2(act)} = CF_{act} \times p1CO_2 \quad (3)$$

364 Where,

365 $CO_{2(act)}$ = respiratory loss from the SOC_{act} pool (g C m⁻²)

366 $p1CO_2$ = scalar that control respiratory CO₂ loss computed as a function of intercept and slope
 367 parameters modified by soil texture

368 The C flow from active to passive pool is then computed as:

$$369 \quad CF_{act2pas} = CF_{act} \times fps1s3 \times (1 + animpt \times (1 - anerb)) \quad (4)$$

370 Where,

371 $CF_{act2pas}$ = C flow from the active to the passive pool (g C m⁻²)

372 $fps1s3$ = impact of soil texture on the C flow (0-1)

373 $animpt$ = the slope term that controls the effect of soil anaerobic condition on C flows from active
 374 to passive pool (0-1)

375 $anerb$ = effect of anaerobic condition on decomposition computed as a function of soil available
 376 water and potential evapotranspiration rates

377 The C flow from active to the slow pool is then computed as the difference between total C flow
 378 out of the active pool, respiratory CO₂ loss, C flow from active to passive pool and C lost due to
 379 leaching. Mathematically,

$$380 \quad CF_{act2slo} = CF_{act} - CO_{2(act)} - CF_{act2pas} - C_{leach} \quad (5)$$

381 Where,

382 C_{leach} = C lost due to leaching calculated as a function of leaching intensity (0-1) and soil texture

383 Likewise, total C flow (CF_{slo}) out of the slow pool is a function of potential decomposition rates
 384 modified by the effect of moisture, temperature, pH, and soil texture.

$$385 \quad CF_{slo} = k_{slo} \times SOC_{slo} \times bg_{dec} \times clt_{slo} \times anerb_{dec} \times pH_{eff} \times dtm \quad (6)$$

386 k_{slo} = intrinsic decomposition rate of the slow pool (yr^{-1})

387 SOC_{slo} = SOC in the slow pool ($g\ C\ m^{-2}$).

388 clt_{slo} = the effect of cultivation on the decomposition rate for crops (0-1) for the slow pool

389 The respiratory loss when the slow pool decomposes is calculated as:

$$390 \quad CO_{2(slo)} = CF_{slo} \times p2CO_2 \quad (7)$$

391 Where,

392 $CO_{2(slo)}$ = respiratory loss from the SOC_{slo} pool ($g\ C\ m^{-2}$)

393 $P2CO_2$ = parameter that controls decomposition rates of the slow pool (0-1)

394 The C flow from slow to passive pool is then computed as:

$$395 \quad C_{slo2pas} = CF_{slo} \times fps2s3 \times (1 + animpt \times (1 - anerb)) \quad (8)$$

396 Where,

397 $fps2s3$ = impact of soil texture on decomposition (0-1)

398 The C flow from slow to active pool is then computed as a difference between total C flow out of
 399 the slow pool, respiratory CO₂ loss and total C flow from slow to passive pool. Mathematically,

$$400 \quad CF_{slo2act} = CF_{act} - CO_{2(slo)} - C_{slo2pas} \quad (9)$$

401 Likewise, total C flow (CF_{pas}) out of the passive pool is a function of potential decomposition rates
 402 modified by the effect of moisture, temperature and pH.

$$403 \quad C_{pas} = k_{pas} \times SOC_{pas} \times bg_{dec} \times clt_{pas} \times pH_{eff} \times dtm \quad (10)$$

404 Where,

405 k_{pas} = intrinsic decomposition rate of the passive pool (yr^{-1})

406 SOC_{pas} = SOC in the slow pool (g C m⁻²).

407 cl_{pas} = the effect of cultivation on the decomposition rate for crops (0-1) for the passive pool

408 The CF_{pas} is either lost through respiratory processes or transferred to the active pool using the
 409 following equation:

$$410 \quad CO_{2(pas)} = CF_{pas} \times p3co2 \quad (11)$$

$$411 \quad CF_{pas2act} = CF_{pas} \times (1 - p3co2) \quad (12)$$

412 Where,

413 $CO_{2(pas)}$ = respiratory loss from the passive SOC pool (g C m⁻²)

414 $p3co2$ = parameter that control decomposition rates of passive pool (0-1)

415 $CF_{pas2act}$ = C flow from passive to active pool (g C m⁻²)

416 Since DAYCENT is a donor-controlled model and changes in organic matter are primarily driven
 417 by a top down approach, we first parameterize the active soil pool by comparing the simulated
 418 SOC in the active pool against POC predicted using diffuse reflectance spectroscopy. During the
 419 parameterization process, we varied the potential decomposition rates (k_{active}) by running the model
 420 to equilibrium under native vegetation for 2000 years. We then used site history at seven long-
 421 term research sites to create schedule files and simulate the effects of historical cropping systems,
 422 land use change, land management and grazing practices on the active SOC. The potential
 423 decomposition rates for the active soil pool were optimized when the absolute difference between
 424 the average of SOC in the active pool and the POC for the top 20 cm across all sites was minimum.
 425 We repeated the above process for parameterizing the slow- and passive-carbon pools by
 426 comparing it with MOAC and PyC, respectively. Similar to the active pool, we performed a grid
 427 search using the existing parameters based on the default model that controls the potential
 428 decomposition rates (k_{slow} and $k_{passive}$) of the slow- and passive-pools. We then optimized the

429 parameter by using the potential decomposition rates that provides the minimum difference in the
430 absolute values across all sites.

431 **2.6 Model calibration and simulation procedure**

432 The DAYCENT model has been well calibrated across a range of climatic, environmental, and
433 land use gradients for different crop and grassland types. Details of the calibration procedure can
434 be found in Hartman et al. (2011). Briefly, adjustment of key model parameters that control plant
435 growth and SOM changes were made by changing the schedule files at each point in time. For
436 example, transitioning to higher yielding corn varieties occurred in 1936, while the short and semi-
437 dwarf wheat varieties were introduced in the 1960s. During the calibration process, model
438 parameters that control the maximum photosynthetic rate and grain to stalk ratio were adjusted
439 within realistic limits to account for improvement in crop varieties. Additionally, adjustments in
440 the schedule files were made to account for residue removal in early years, while residues were
441 retained in later years, thereby increasing nutrient input to the soils. These calibration strategies
442 have allowed to better capture crop dynamics in the US Great Plains region (Hartman et al., 2011).
443 Model simulation begins with the equilibrium run starting from year zero to year 1894 by repeating
444 daily climate data from 1895-2005 and native vegetation without disturbance or land use change.
445 Following the equilibrium run, we performed a historical simulation to quantify the effects of land
446 use history, land management practices, and climate change on the evolution of SOC during 1895-
447 2005. Finally, we performed future simulations using two climate scenarios (RCP4.5 and RCP8.5)
448 and A2 LCLUC, with land management practices (i.e. irrigation, fertilization, tillage practices, and
449 crop rotation) held at 2005 levels during 2006-2100.

450 **2.7 Model validation at site and regional scales**

451 The performance of the calibrated model was assessed by comparing simulated SOC in the active,
452 slow, and passive pools against predictions of POC, MAOC and PyC, respectively, at the seven
453 long-term research sites. In the validation procedure, we ran the model at these sites using plant
454 growth and soil parameters determined from model calibration, but with changing climate,
455 environmental, and land use data based on the land use history of the respective sites. For all the
456 sites, we compared the distribution of SOC in different pools and evaluated model performance
457 using linear regression and the goodness-of-fit statistics (bias, R^2 , RMSE).

458 We also compared the distribution of SOC simulated using DAYCENT against the machine
459 learning model-based predictions of POC, MAOC, and PyC for the US Great Plains ecoregion
460 (Sanderman et al., 2021). Additionally, we compared simulated total SOC against two other SOC
461 maps for the contemporary period (Hengl et al., 2017; Ramcharan et al., 2018) .

462 **2.8 Historical and future changes in SOC stocks**

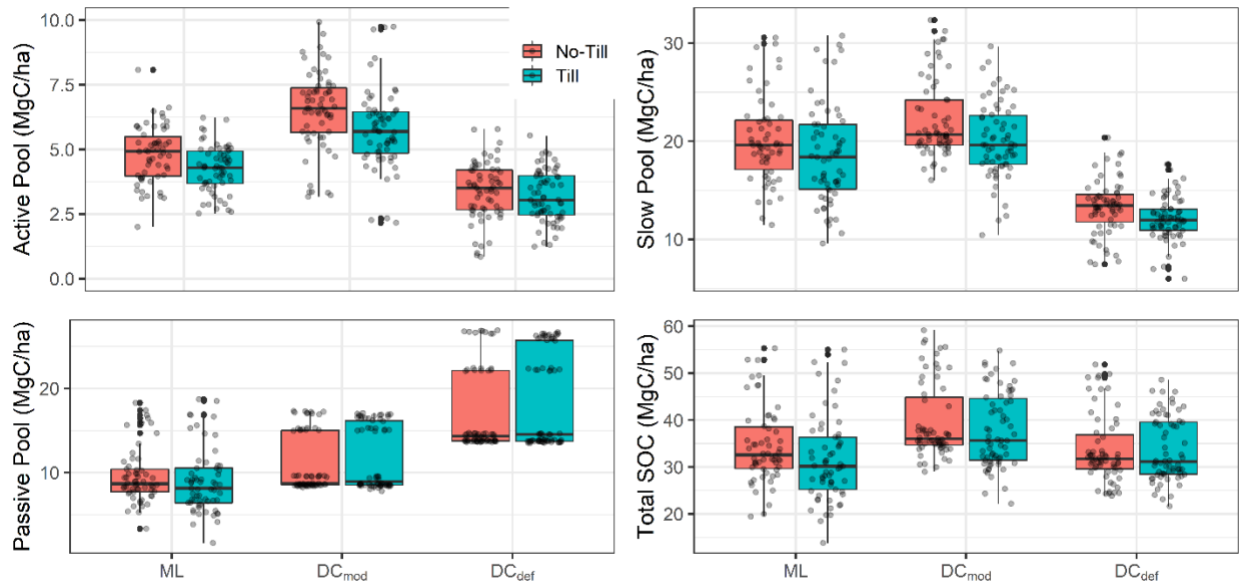
463 To quantify the effect of the new parameterization scheme linking measurable soil C pools with
464 conceptual active, slow, and passive pools from the DAYCENT, we designed two scenarios. In
465 the first scenario, we ran the model using the default (DC_{def}) and the modified (DC_{mod}) model that
466 links conceptual pools with C fraction during the historical period (1895-2005) to quantify the
467 differences in SOC across different pools associated with different parameterization. In the second
468 scenario, we performed future simulations to understand if the different model structures (DC_{def}
469 versus DC_{mod}) result in different effects of climate and LCLUC on SOC stocks. We used the IPCC
470 AR5 RCP8.5 and RCP4.5 climate scenarios and the IPCC AR4 A2 LCLUC scenarios to quantify
471 the effects of future climate and LCLUC change on SOC stocks. The RCP8.5 corresponds to the
472 pathway that tracks current global trajectories of cumulative CO_2 emissions (CO_2 levels reaching

473 960 ppm by 2100) with the assumption of high population growth and modest rates of
474 technological change and energy intensity improvements (Riahi et al., 2011; Schwalm et al., 2020).
475 The RCP4.5 is a modest emission scenario with CO₂ levels reaching 540 ppm by 2100 under the
476 assumption of shift toward low emission technologies and the deployment of carbon capture and
477 geologic storage technology (Thomson et al., 2011). The A2 land cover scenario emphasizes rapid
478 population growth and economic development, and resembles closely to the RCP8.5 scenario. We
479 used the AR4 for LCLUC because Sohl et al. (2012) data were available at high resolution and
480 allowed for smoother transition between land cover types when moving from historical to future
481 A2 LCLUC scenarios. The purpose of the second scenario is to better understand the response of
482 SOC to future climate and LCLUC and examine the effect of the new model modification on the
483 projected change in total SOC through 2100.

484 **3. Results and Discussion**

485 By quantifying the size and distribution of conceptual SOC pools of ecosystem models using a
486 combination of diffuse reflectance spectroscopy and machine learning, we were able to modify
487 DAYCENT by relating the conceptual active, slow and passive pools with measurable POC,
488 MAOC and PyC fractions (section 3.1). Model modification led to more accurate representation
489 of the magnitude and distribution of SOC (section 3.2) and was necessary to accurately quantify
490 the legacy effect of previous land use under a changing climate and reproduce current SOC
491 stocks compared to the default model (section 3.3). Projection of future SOC change show that
492 the default model underestimates the SOC loss in response to climate and land cover change by
493 31% and 29% for croplands and grasslands, respectively (section 3.4). Overall, our results
494 demonstrate that relating the pools sizes from the ecosystem model with C fraction data is

495 necessary to better initialize SOC pool and simulate SOC response to climate and land use into
 496 the future.

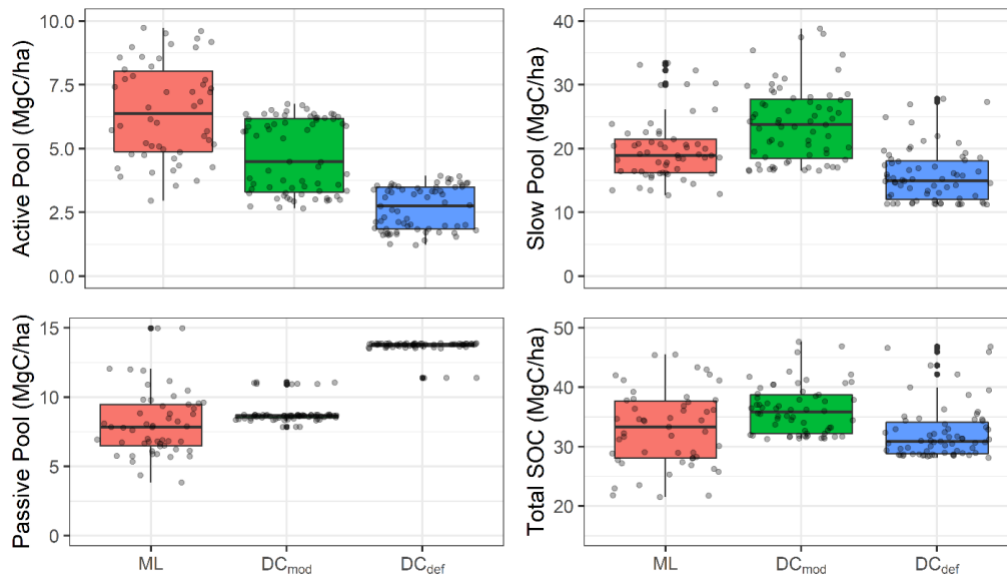


497
 498 **Figure 2.** Comparison of the machine learning (ML) and DAYCENT simulated SOC using the
 499 modified (DC_{mod}) and default (DC_{def}) models at long-term research sites with a known cropping
 500 history. The black dots in the boxplot represent the SOC at the various sites plotted by adding a
 501 random value such that they do not overlap with each other.

502 3.1 Model evaluation of total SOC and the distribution of SOC at long-term research sites

503 The modified model (DC_{mod}) linking conceptual soil pools to measurable C fractions showed better
 504 representation of the distribution of C stocks across different pools compared to the default model
 505 (DC_{def}) (Figures 2 & 3). When the mean SOC at these sites were compared to DC_{mod} and DC_{def}
 506 simulated SOC, DC_{mod} had better fit ($R^2 = 0.52$) and lower RMSE ($8.49 \text{ Mg C ha}^{-1}$) compared to
 507 DC_{def} ($R^2 = 0.40$; RMSE = $8.93 \text{ Mg C ha}^{-1}$) (Figure S5). The mean SOC based on observation for
 508 these sites was $38.96 \text{ Mg C ha}^{-1}$, which is comparable to the sum of predicted C fractions (37.07
 509 Mg C ha^{-1}) and simulated SOC using DC_{mod} ($42.30 \text{ Mg C ha}^{-1}$) and DC_{def} ($36.60 \text{ Mg C ha}^{-1}$)
 510 models. The DC_{mod} simulated SOC was higher than observation and machine learning based SOC

511 by 9 and 12%, respectively, while DC_{def} showed under-predicted SOC by 6% compared to
 512 observation. Although DC_{mod} showed a tendency toward over-prediction, assessment of the
 513 distribution of SOC demonstrated that DC_{mod} was able to better simulate the distribution of SOC
 514 in soil pools compared to DC_{def} . The DC_{mod} simulated the highest proportion of C in the slow
 515 (56%) pool followed by the passive (30%) and active (14%) pools, which is comparable to the
 516 machine learning model-based estimates of MAOC (57%), PyC (29%) and POC (14%),
 517 respectively. Unlike DC_{mod} , DC_{def} model simulated the highest proportion of C in passive (53%),
 518 followed by slow (39%) and active (8%) pools (Table S2).



519
 520 **Figure 3.** Comparison of the machine learning (ML) and DAYCENT simulated SOC using the
 521 modified (DC_{mod}) and default (DC_{def}) models across different pools at two long-term research sites
 522 dominated by grasslands with a known grazing history. The black dots in the boxplot represent the
 523 SOC across different sites plotted by adding a random value such that they do not overlap with
 524 each other.

525 Evaluation of the model performance (DC_{mod}) for grasslands and croplands showed that the
 526 modified model (DC_{mod}) outperformed the default model (DC_{def}) with better model fit ($R^2 = 0.60$),

527 lower bias ($-1.94 \text{ Mg C ha}^{-1}$) and lower RMSE (6.7 Mg C ha^{-1}) for grasslands (Figure S6). The
528 DC_{mod} also produced better model fit for croplands ($R^2 = 0.48$), but higher bias ($-5.84 \text{ Mg C ha}^{-1}$)
529 and RMSE ($8.86 \text{ Mg C ha}^{-1}$) compared to the default (DC_{def}) model (bias = -0.82 and RMSE =
530 $7.45 \text{ Mg C ha}^{-1}$). The DC_{mod} was able to better represent the distribution of C in the active, slow
531 and passive pools for both grasslands and croplands, while DC_{def} showed large discrepancies when
532 representing the distribution of SOC for croplands (Table S2).

533 The results of this exercise demonstrate that optimizing the model parameters to initialize the
534 conceptual SOC pools by matching with C fraction data can reproduce the distribution of SOC
535 (Figures 2 & 3), building confidence in the modeling of SOC stocks, and their pool distribution
536 (Lee and Viscarra Rossel, 2020; Luo et al., 2016). A common approach to initializing soil C pools
537 is based on the use of soil C steady-state conditions, which is primarily achieved by running the
538 model over a long period of 100 to 10000 years under native vegetation. However, this approach
539 has shown large uncertainty in the estimation of contemporary SOC partly due to differences in
540 parameter values used to determine the initial SOC stocks, which vary many fold across models
541 (Tian et al., 2015; Todd-Brown et al., 2014). Additionally, the size and distribution of the soil C
542 pools are constrained by model structure and parameter values producing large differences in
543 initial conditions, which ultimately propagates into uncertainties in historical and future projection
544 of SOC change (Ogle et al., 2010; Shi et al., 2018). Relating these conceptual pools to measurable
545 C fractions by optimizing parameters that control decomposition rates can help to constrain initial
546 pool size and reduce uncertainties related to initial SOC stocks across different models
547 (Christensen, 1996; Luo et al., 2016; Zimmermann et al., 2007). Results of this study show that
548 tuning the potential decomposition rates within reasonable range (Figure 1) can effectively capture

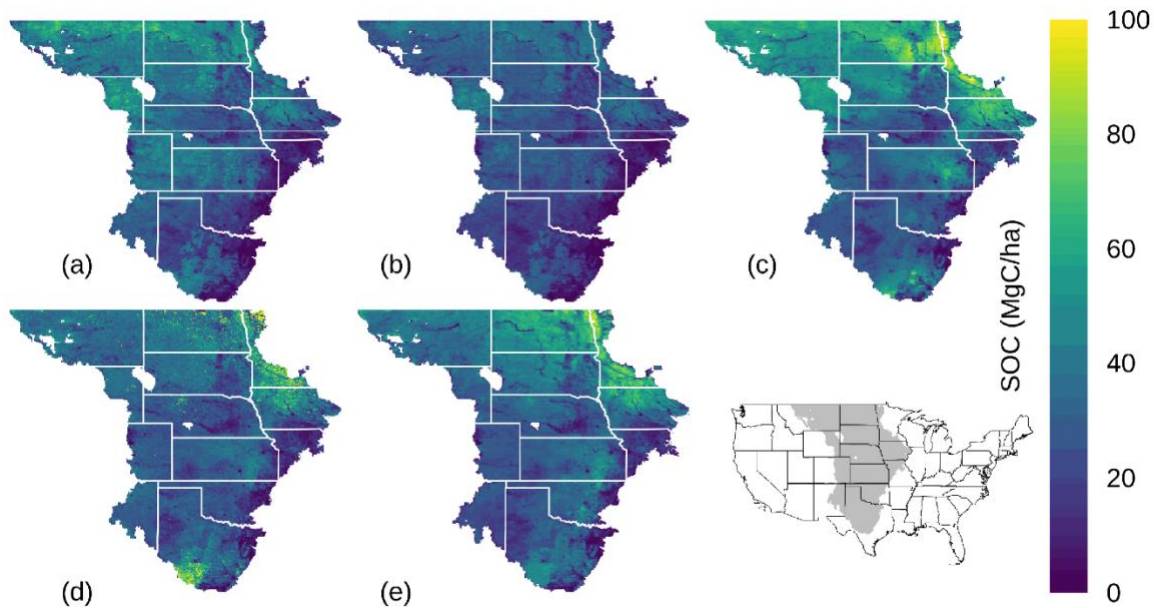
549 the distribution of SOC among different pools without significantly altering the magnitude of total
550 SOC (Figures 2 & 3).

551 While tuning the parameters that control potential decomposition rates, active, and slow pools
552 were adjusted by -3.8 yr^{-1} (-52% compared to default rate) and -0.06 yr^{-1} (-30%) respectively, and
553 passive pool was increased by 0.003 yr^{-1} (67%) to match with C fractions data at the long-term
554 research sites. These modifications were done such that the model was able to simulate total SOC
555 and their distribution under current climatic, and land use conditions while also allowing to capture
556 the legacy effect of previous land use, crop rotation, and tillage practices. It is important to note
557 that other soil C models use C fraction data obtained under land use of varying intensities to run
558 the model to steady state (Zimmermann et al., 2007), although soils under continuous use are in a
559 transient state (Wieder et al., 2018). The rate and direction of SOC change can be modified by
560 environmental factors, previous land use, and current management practices (e.g., intensity,
561 cropping systems and fertilization/irrigation), which ultimately determine a new equilibrium or
562 transient state (Chan et al., 2011; Van Groenigen et al., 2014). Here, we run the model to steady
563 state conditions, and calibrated the SOC stocks to current land use and management practices by
564 matching with C fractions data at all the sites.

565 **3.2 Model evaluation of SOC stocks and their distribution at the regional scale**

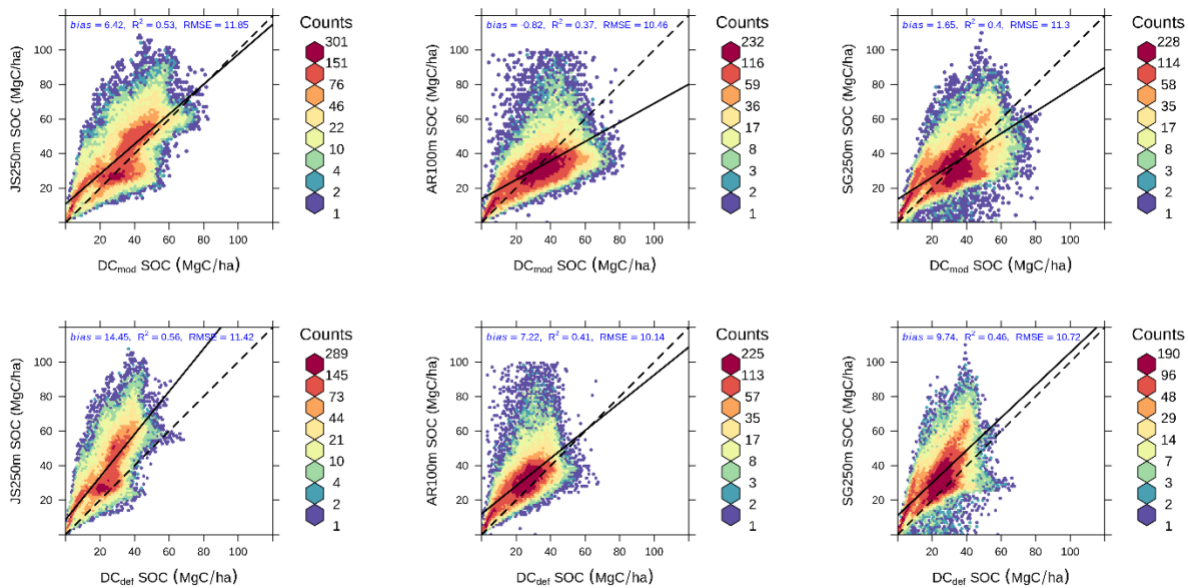
566 Evaluation of the model performance at the regional level by comparing model simulations to three
567 data-driven SOC maps showed that the default (DC_{def}) model under-predicts SOC stocks for the
568 contemporary period (2001-2005 average). The modified (DC_{mod}) model was better able to
569 reproduce the spatial pattern as observed in the data driven estimates of SOC (Figure 4). The DC_{mod}
570 simulated contemporary SOC stocks of $34.86 \text{ Mg C ha}^{-1}$ were closer to the estimates based on
571 three data-driven models ($32.38 - 39.19 \text{ Mg C ha}^{-1}$) (Figure S7). The DC_{def} simulated SOC stocks
572 of $26.17 \text{ Mg C ha}^{-1}$, which is lower than the machine learning based predictions by 19-33%.

573 Interestingly, both DC_{def} and DC_{mod} were not able to reproduce the high C stocks in the
 574 northeastern Great Plains although data driven modeling shows large SOC stocks.



575
 576 **Figure 4.** Spatial pattern of SOC change during the contemporary period: modified (DC_{mod}) (a),
 577 default (DC_{def}) (b), Sanderman et al. (2021) (c), Ramcharan et al. (2018) (d), and Hengl et al.
 578 (2017) (e). Data-driven SOC maps were scaled by cropland and grassland distribution maps before
 579 comparing against DAYCENT-simulated SOC.

580 Evaluation of the model performance using a scatterplot shows that calibration of active, slow, and
 581 passive pools was necessary to produce unbiased estimates of SOC despite having slightly higher
 582 RMSE values than the default model when compared to the different SOC data sets (Figure 5).
 583 Among the three data driven models, Sanderman et al. (2021) also provided prediction of POC,
 584 MAOC, and PyC in the US Great Plains region. Comparison of the distribution of SOC across
 585 different pools indicate that the DC_{mod} was able to reproduce SOC in the slow/MAOC, and
 586 passive/PyC pools but under-predicted the size of the active/POC pool (Figure S8).



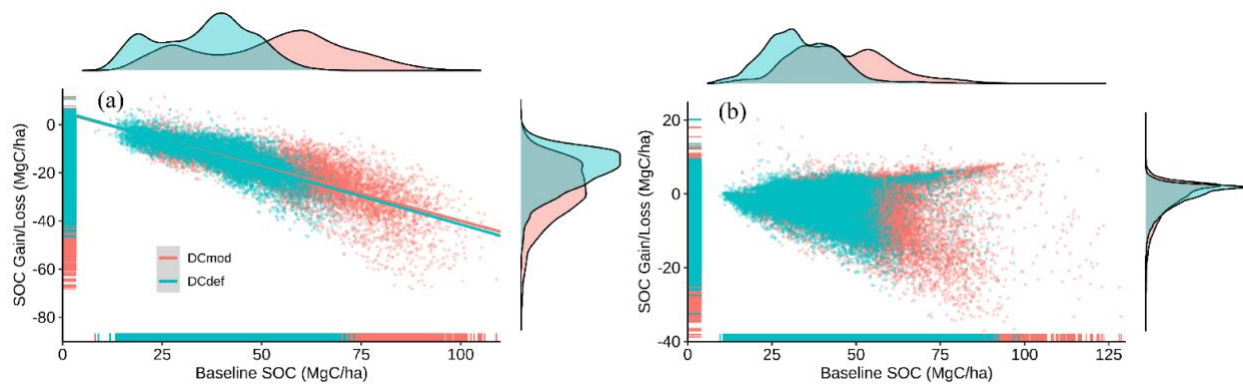
587
 588 **Figure 5.** Scatter plots of the comparison of DAYCENT simulated SOC (DC_{mod} & DC_{def}) against
 589 Sanderman et al. (2021) – JS250m, Ramcharan et al. (2018) – AR100m, and Hengl et al. (2017) –
 590 SG250m.

591 While the modified (DC_{mod}) model was able to better capture the magnitude and spatial pattern of
 592 SOC when compared against data based on machine learning models, the datasets themselves
 593 present a few challenges when comparing with the results from this study. First, these datasets
 594 were produced using the environmental covariates approach under current climatic and land use
 595 conditions, and thus represent SOC dynamics using aggregated climate, land use, and
 596 environmental conditions over a certain period. However, in the DAYCENT model, we used
 597 annual and daily time series data for climatic and land use conditions to simulate the processes that
 598 control SOM retention and stabilization, which could lead to inconsistencies when comparing
 599 results between this study and data driven products. Second, outputs based on machine
 600 learning models are sensitive to the number of samples used in the training sets. For example, machine
 601 learning-based SOC shows higher stocks in the northeastern Great Plains region compared to the
 602 DC_{mod} or DC_{def} models (Figure 4). This may be because the region contains thousands of shallow

603 seasonal wetlands with higher SOC stocks averaging between 78 to 109 Mg C ha⁻¹ to the depth of
604 20cm (Tangen and Bansal, 2020). Accounting for the large number of wetlands samples in the
605 training set would likely produce higher SOC stocks in the region. We did not specifically model
606 wetlands SOC and only considered grasslands and croplands, which cover >90% of the land area
607 in the US Great Plains region and as such may have underrepresented these high SOC ecosystems.

608 **3.3 Historical changes in SOC stocks and their distribution**

609 When the baseline SOC (1895-1899 average) values were compared with the current (2001-2005
610 average) SOC stocks, the modified (DC_{mod}) and default (DC_{def}) models simulated a loss of 1063
611 Tg C (12%) and 634 Tg C (10%), respectively. On a per unit area basis, DC_{mod} showed higher
612 absolute (17.62 Mg C ha⁻¹) and relative (33%) SOC losses compared to the loss of 10.60 Mg C ha⁻¹
613 (27%) using DC_{def} for croplands. Grasslands showed similar patterns of higher absolute (2.51
614 Mg C ha⁻¹) and relative (4%) SOC losses using DC_{mod} compared to the loss of 1.06 Mg C ha⁻¹
615 (3%) using DC_{def}. Overall, croplands showed a large and significant loss of C when compared
616 against the baseline SOC using both models, while grasslands showed both losses and gains of
617 SOC during 1895-2005 (Figure 6). The SOC loss from conversion of native vegetation to
618 croplands were on average 14.70 Mg C ha⁻¹ and 9.29 Mg C ha⁻¹ using DC_{mod} and DC_{def},
619 respectively. This translates into a relative loss using DC_{mod} that is higher than the loss using DC_{def}
620 by 58% during 1895-2005. For grid cells under native grasslands, DC_{mod} simulated slightly higher
621 average SOC loss (1.96 Mg C ha⁻¹) compared to DC_{def} (1.39 Mg C ha⁻¹).

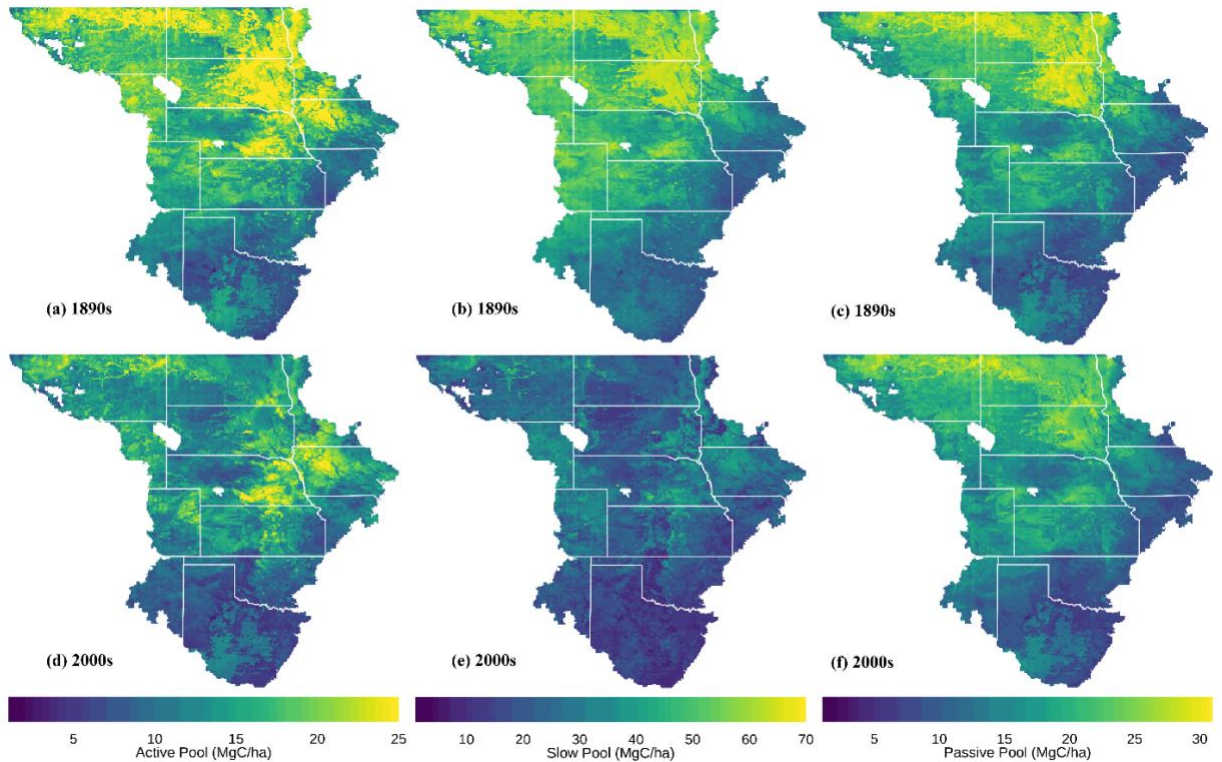


622

623 **Figure 6.** Changes in contemporary (2001-2005 average) SOC after conversion of native
 624 vegetation to croplands (a) and under native vegetation (b) as a function of baseline (1895-1899
 625 average) SOC stocks. Negative values are losses while positive values are gains of SOC.

626 The simulation of total SOC stocks following historical land use under a changing climate is
 627 constrained by model parameters that determine the time until decomposition, modified by the
 628 interaction of land use intensity with changing climate (Arora and Boer, 2010; Eglin et al., 2010).
 629 Land use change can modify total SOC through its effect on individual soil pools, with the
 630 POC/active pool more vulnerable to loss compared to the MAOC/slow and PyC/passive pools
 631 (Poeplau and Don, 2013). The potential decomposition rates using the modified (DC_{mod}) model
 632 were adjusted to match C fraction data such that higher SOC was allocated to rapid and slow
 633 cycling pools, which are more vulnerable to loss following land use change and management
 634 intensity at decadal to century time scales (Hobley et al., 2017; Sulman et al., 2018). We further
 635 compared the historical SOC loss following land use change against other studies to determine the
 636 robustness of the new parameterization using DC_{mod}. The SOC loss rate using DC_{mod} are closer to
 637 the mean 30 cm loss rate of 17.7 Mg C ha⁻¹ (Sanderman et al., 2017b), and relative loss of 42-49%
 638 following conversion of forest/pasture to croplands (Guo and Gifford, 2002). However, it is
 639 important to note that these previous studies are not directly comparable with the results from this

640 study because of differences in sampling depth, the intensity of land use and the time since
 641 disturbance.



642

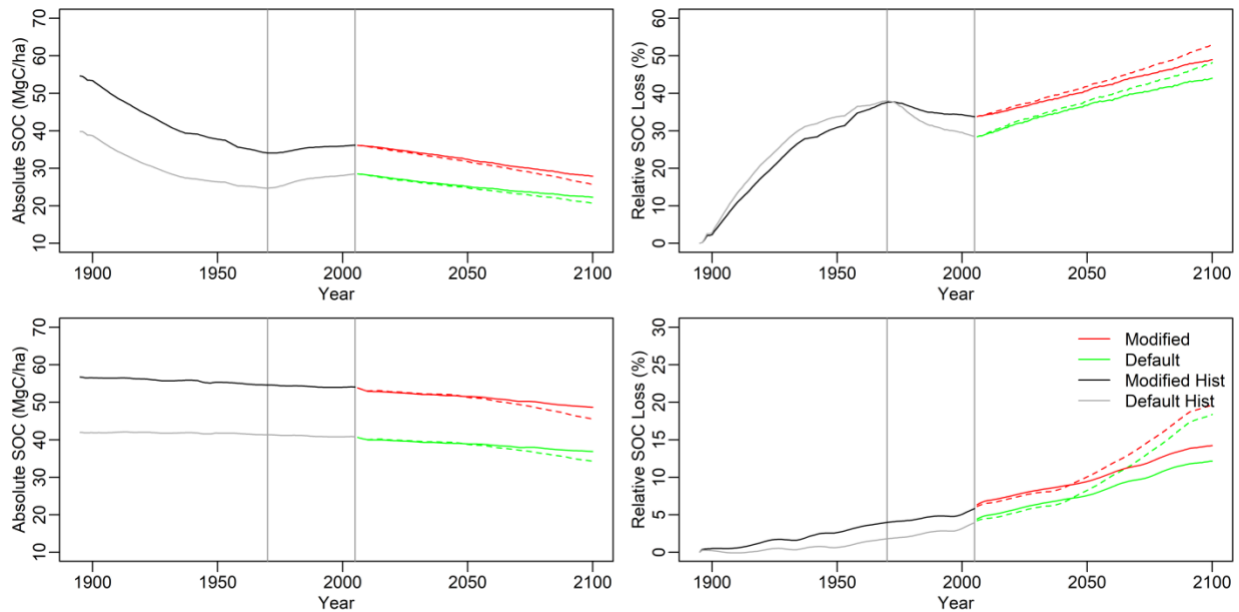
643 **Figure 7.** The active, slow, and passive soil pools of SOC stocks (20 cm depth) based on the
 644 modified (DC_{mod}) model under native vegetation (1895-1899 average; top maps) and following
 645 land cover land use change (2001-2005 average; bottom maps).

646 Comparison of the total SOC and its distribution in different pools between the two models
 647 provided a more nuanced picture of the effect of new parameterization on SOC stocks and the
 648 response of SOC to historical land use. The spatial pattern of the SOC stocks showed that the
 649 baseline SOC in the active, slow and passive pools simulated by the modified (DC_{mod}) model
 650 (Figure 7) were higher than the default (DC_{def}) model (Figure S9). As a result, there were higher
 651 SOC losses from the active and slow pools using DC_{mod} compared to DC_{def} (Figure 7, S9). When
 652 averaged over all pixels, the cropland SOC loss in the active, and slow, pools were 0.85, 10.09 and

653 gains in the passive pool was $0.34 \text{ Mg C ha}^{-1}$, respectively, using DC_{def} . The DC_{mod} simulated
654 larger SOC loss for all pools with active, slow, and passive pools losing SOC by 1.48, 16.04 and
655 $0.09 \text{ Mg C ha}^{-1}$, respectively. The magnitude of SOC loss from grasslands was lower compared to
656 croplands for all three pools, with the largest SOC loss from the slow pool of 1.45 and 0.49 Mg C
657 ha^{-1} using DC_{mod} and DC_{def} models, respectively. The distribution of SOC to different pools
658 indicated that DC_{def} had 44%, 43% and 13% SOC in the passive, slow, and active pools for
659 croplands, while DC_{mod} had 57% of the total SOC allocated to the slow pool, followed by the
660 passive (23%) and active (20%) pools. For grasslands, both models were consistent in allocating
661 the largest proportion of SOC (59% in default and 70% in modified) to slow pools, followed by
662 passive and active pools.

663 The differences in the total SOC and their distribution between the models is constrained by the
664 sensitivity of the SOC pools to environmental, climatic, and management factors (Davidson and
665 Janssens, 2006; Dungait et al., 2012; Luo et al., 2016). The SOC stocks in the passive pool are not
666 significantly different between the models at the regional level because the passive pool is less
667 sensitive to environmental, climatic, and management factors, and it has a smaller contribution to
668 total SOC (Collins et al., 2000), the SOC stocks in the passive pool were not significantly different
669 between the models at the regional level. However, the active and slow pools respond strongly to
670 environmental, climatic, and management constraints, which is largely driven by rapidly cycling
671 fresh organic matter input in the active pool, and gradually decomposing detritus in the slow pool
672 (Sherrod et al., 2005). In the DC_{mod} , the potential decomposition rates of the active and slow pools
673 are adjusted, allowing the model to retain more SOC to match with C fraction data. This
674 modification resulted in higher SOC stocks in these pools, which translated into higher total losses
675 despite slower turnover rates relative to DC_{def} . Model modification was necessary not only to

676 match total SOC values but also to simulate the distribution of SOC into the active, slow and
 677 passive pools.



678
 679 **Figure 8.** Temporal change in the absolute SOC stocks (20 cm depth) for croplands (a) and
 680 grasslands (c) and relative SOC loss compared to the 1895 SOC for croplands (b) and grasslands
 681 (d) in response to land use under a changing climate through 2100. The solid and dashed lines after
 682 2006 represent RCP4.5 and RCP8.5 climate scenarios, respectively, both under the A2 land cover
 683 change scenario.

684 3.4 Future changes in SOC stocks and their distribution

685 Projection of the SOC dynamics in response to land cover change under a changing climate
 686 resulted in greater relative changes for both croplands and grasslands using the modified (DC_{mod})
 687 compared to the default (DC_{def}) model (Figure 8). Despite greater rates of loss, by the end of the
 688 21st century, DC_{mod} still simulated higher total SOC stocks compared to DC_{def} model (Table 3).
 689 By the end of 21st century, the DC_{mod} simulated total SOC stocks of 2818 and 2563 Tg C for
 690 croplands under the RCP4.5 and RCP8.5 scenarios, while the DC_{def} simulated total SOC stocks of

691 2266 and 2082 Tg C. Native grasslands had higher SOC stocks of 3310 and 3095 Tg C using the
692 DC_{mod} compared to the SOC stocks of 2505 and 2324 Tg C using the DC_{def} under the RCP4.5 and
693 RCP8.5 scenarios, respectively. On a per unit area basis, absolute loss (difference between the
694 2095s and 2000s) were slightly higher for croplands, with a mean loss rate $10.43 \text{ Mg C ha}^{-1}$
695 compared to $8.44 \text{ Mg C ha}^{-1}$ for grasslands using DC_{mod} under the RCP8.5 scenario (Table 3). The
696 DC_{def} also simulated similar trend with slightly higher absolute losses for croplands (7.85 Mg C
697 ha^{-1}) compared to grasslands ($6.55 \text{ Mg C ha}^{-1}$) under the RCP8.5 scenario. Relative losses
698 estimated as a percentage of contemporary SOC stocks were higher in croplands (29% for DC_{mod}
699 vs 28% for DC_{def} model) compared to grasslands (16% for both DC_{mod} and DC_{def} model) under
700 the RCP8.5 scenario. Using the DC_{mod} , the SOC loss rate were 33% and 29% higher for croplands
701 and grasslands, respectively, compared to the DC_{def} by the end of the 21st century under the RCP8.5
702 scenario. While both models simulated total SOC loss over the 21st century, the difference in SOC
703 between models sums to an additional loss of 1252 Tg SOC under the RCP8.5 scenario.

704 The turnover rates of SOM are primarily driven by temperature and environmental controls with
705 significant impact on the dynamics of total SOC changes at decadal to century time scales (Knorr
706 et al., 2005). The two model versions used the same climate and environmental data and only differ
707 in the turnover rates of the active, slow, and passive pools. Because the sizes of active, and slow
708 pools in the modified (DC_{mod}) model were larger than the default (DC_{def}) model, simulated
709 absolute and relative losses were higher using the DC_{mod} compared to the DC_{def} for croplands.
710 Larger losses using the DC_{mod} are primarily associated with the legacy effects of management
711 intensity and rising temperatures with larger rates of SOC loss from the active, and slow pools
712 (Crow and Sierra, 2018) of DC_{mod} compared to DC_{def} . Additionally, the size of the passive pool in
713 DC_{def} is larger compared to DC_{mod} , and this pool is less vulnerable to land use intensity and

714 warming climate compared to active and slow pools. Thus, there was a disproportionately larger
715 SOC loss driven by the size of the slow pool and the interaction of climate and management
716 intensity using the DC_{mod} compared to the DC_{def} , which translated into larger absolute and relative
717 losses of SOC. For grasslands, we did not include any management driven changes. Both absolute
718 and relative losses of SOC stocks in the grasslands are primarily driven by the warming climate
719 (Jones and Donnelly, 2004), with active and slow pools losing more SOC stocks using DC_{mod}
720 compared to DC_{def} . Future work should consider the interactive effects of grazing management
721 with climate.
722

723
724**Table 3.** DAYCENT (modified and default) simulated absolute changes in total and per unit area soil organic carbon (SOC) during the 2000s, 2045s and 2095s for croplands and grasslands in the US Great Plains region

Time	Total (TgC)						Per Unit Area (MgC/ha)																					
	Default (DC _{def})		Modified (DC _{mod})		Default (DC _{def})		Modified (DC _{mod})		Default (DC _{def})		Modified (DC _{mod})																	
	RCP4.5	RCP8.5	RCP4.5	RCP8.5	RCP4.5	RCP8.5	RCP4.5	RCP8.5	RCP4.5	RCP8.5	RCP4.5	RCP8.5																
Croplands	2000s	2113		2717		28.51		36.17		2045s	1988		2513		25.20		32.41		2095s	2266		2563		22.31		27.91		25.87
Grasslands	2000s	3891		5160		40.82		54.05		2050s	3531		4674		38.90		51.51		2095s	2505		3095		36.88		48.65		45.61
Total	2000s	6004		7877		NA		NA		(Croplands + Grasslands)	5519		7172		NA		NA		2095s	4771		5658		NA		NA		NA

725 Future land use, management intensity, nitrogen content, and climate interact in different ways to
726 control C flow from soil pools with different mean residence times, which ultimately determine
727 total SOC stocks (Deng et al., 2016; Luo et al., 2017; Sulman et al., 2018). Under a warming
728 climate, SOC formed from fresh organic matter inputs controls the size of the active/POC pool,
729 which is further constrained by the intensity of land use and is more vulnerable to loss (Crow and
730 Sierra, 2018; Lavalley et al., 2020). The active/POC pool also acts as a donor to the slow/MAOC
731 pool with C transfer and rates of SOC accumulation increasingly controlled by temperature (Crow
732 and Sierra, 2018). In the DAYCENT, regardless of model version, the size of the active pool is
733 relatively small as fresh organic matter is either decomposed rapidly or quickly enters the slow
734 pool. Because the slow pool has longer residence times ranging from years to decades, the slow
735 pool is less vulnerable to loss and can accrue C when transfer rates from the active pool exceed
736 the rates of decomposition (Collins et al., 2000; Fontaine et al., 2007). In this study, the rates of
737 decomposition due to rising temperatures had a stronger control on the size of the slow pool
738 compared to the transfer of SOC from the active pool. As a result, the slow pool continued to lose
739 SOC under projected climate changes in the future.

740 **4 Conclusions**

741 In this study, we developed an approach to link conceptual soil pools in biogeochemical models
742 against C fraction data predicted using a combination of diffuse reflectance spectroscopy and
743 machine learning. We then quantified the long-term evolution of SOC change and projected the
744 SOC response to future climate and land cover scenarios using the modified (DC_{mod}) model that
745 has been calibrated to C fraction data. Our results demonstrate that matching the active, slow and
746 passive pools against POC, MOAC and PyC data lead to better representation of total SOC stocks
747 and the distribution of SOC into different pools. With the updated model, the long-term legacy

748 effect of past agricultural management results in larger absolute and relative losses of SOC
749 compared to the default (DC_{def}) model. Projecting the SOC response to climate and land cover
750 change into the future (2005-2100) indicates that the new model modification (DC_{mod}) increases
751 SOC losses by 2100 by 32% and 28% for croplands and grasslands, respectively, under the RCP8.5
752 scenario compared to using the DC_{def} model.

753 There are several study limitations that need to be addressed in our future work. First, new
754 modeling efforts should also consider quantifying how changes in aboveground biomass inputs
755 quantity and quality affect SOC dynamics given mixed results in agricultural systems in response
756 to litter inputs (Halvorson et al., 2002; Sanderman et al., 2017a). Second, current models rely on
757 using clay content to modify rates of SOM stabilization and turnover, but recent research has
758 shown that other soil physicochemical properties such as exchangeable calcium and extractable
759 iron and aluminum are stronger predictors of SOM content (Rasmussen et al., 2018). Third, new
760 modeling efforts should constrain model parameters affecting SOC dynamics by integrating them
761 with data-driven modeling and long-term experimental data (Jandl et al., 2014). Finally, given the
762 paucity of data related to C fractions, there is increasing need for measurement and modeling of C
763 fractions across a wide range of environmental and management gradients (Luo et al., 2017).
764 Despite these limitations, we have shown that models calibrated to pool sizes by matching with C
765 fractions can improve long-term SOC predictions by more accurately representing soil C
766 transformations in response to climate, land cover and land use change.

767 **Code and Data Availability:**

768 The DAYCENT model source code is available in Harvard dataverse repository
769 (<https://dataverse.harvard.edu/dataverse/daycent45>). The new parameterization scheme and
770 scripts for regional model simulation are available in github (<https://github.com/whrc/DAYCENT->

771 [soil-carbon-pools](#)). Input data for driving the models are freely available online from different
772 sources and have been cited appropriately in the manuscript. Long term ecological data are part of
773 United States Department of Agriculture – Agricultural Research Service and can be requested
774 from the references listed in Table 1.

775 **Author Contributions:** S.D., C.S, and J.S designed the study and model development. S.D.
776 performed model improvement, calibration, validation and regional historical and future
777 simulation. All authors contributed to the manuscript.

778 **Competing Interest:** The authors declare that they have no conflict of interest.

779 **Acknowledgements**

780 Funding for this research was provided by USDA NIFA award #2017-67003-26481. We thank
781 Melannie D Hartman at Colorado State University for providing access to the DAYCENT model
782 and help with running the model. We also thank staff at the USDA National Soil Survey Center
783 (NSSC) Kellogg Soil Survey Laboratory (KSSL) for providing access to the soil characterization
784 database. This research also used data from the Long-Term Agroecosystem Research (LTAR)
785 network and Columbia Plateau Conservation Research Center (CPCRC), which are both supported
786 by the United States Department of Agriculture. The NSF Long-term Ecological Research
787 Program (DEB 1832042) and Michigan State University AgBioResearch provided funding for the
788 data and soil samples from the Kellogg Biological Station.

789 **References**

- 790 Arora, V.K., Boer, G.J., 2010. Uncertainties in the 20th century carbon budget associated with land use
791 change. *Global Change Biology* 16, 3327–3348.
- 792 Baker, N.T., 2011. Tillage Practices in the Conterminous United States, 1989-2004—datasets Aggregated
793 by Watershed. US Department of the Interior, US Geological Survey Reston, Virginia.
- 794 Baldock, J.A., Hawke, B., Sanderman, J., Macdonald, L.M., 2013a. Predicting contents of carbon and its
795 component fractions in Australian soils from diffuse reflectance mid-infrared spectra. *Soil
796 Research* 51, 577–595.
- 797 Baldock, J.A., Sanderman, J., Macdonald, L.M., Puccini, A., Hawke, B., Szarvas, S., McGowan, J., 2013b.
798 Quantifying the allocation of soil organic carbon to biologically significant fractions. *Soil
799 Research* 51, 561–576.
- 800 Basso, B., Gargiulo, O., Paustian, K., Robertson, G.P., Porter, C., Grace, P.R., Jones, J.W., 2011.
801 Procedures for initializing soil organic carbon pools in the DSSAT-CENTURY model for agricultural
802 systems. *Soil Science Society of America Journal* 75, 69–78.
- 803 Batjes, N.H., 2016. Harmonized soil property values for broad-scale modelling (WISE30sec) with
804 estimates of global soil carbon stocks. *Geoderma* 269, 61–68.
- 805 Cagnarini, C., Renella, G., Mayer, J., Hirte, J., Schulin, R., Costerousse, B., Della Marta, A., Orlandini, S.,
806 Menichetti, L., 2019. Multi-objective calibration of RothC using measured carbon stocks and
807 auxiliary data of a long-term experiment in Switzerland. *European Journal of Soil Science* 70,
808 819–832.
- 809 Carvalhais, N., Forkel, M., Khomik, M., Bellarby, J., Jung, M., Migliavacca, M., Saatchi, S., Santoro, M.,
810 Thurner, M., Weber, U., 2014. Global covariation of carbon turnover times with climate in
811 terrestrial ecosystems. *Nature* 514, 213–217.
- 812 Cavigelli, M.A., Teasdale, J.R., Conklin, A.E., 2008. Long-term agronomic performance of organic and
813 conventional field crops in the mid-Atlantic region. *Agronomy Journal* 100, 785–794.
- 814 Chan, K.Y., Conyers, M.K., Li, G.D., Helyar, K.R., Poile, G., Oates, A., Barchia, I.M., 2011. Soil carbon
815 dynamics under different cropping and pasture management in temperate Australia: Results of
816 three long-term experiments. *Soil Research* 49, 320–328.
- 817 Christensen, B.T., 1996. Matching measurable soil organic matter fractions with conceptual pools in
818 simulation models of carbon turnover: revision of model structure. *Evaluation of soil organic
819 matter models* 143–159.
- 820 Ciais, P., Sabine, C., Bala, G., Bopp, L., Brovkin, V., Canadell, J., Chhabra, A., DeFries, R., Galloway, J.,
821 Heimann, M., 2014. Carbon and other biogeochemical cycles, in: *Climate Change 2013: The
822 Physical Science Basis. Contribution of Working Group I to the Fifth Assessment Report of the
823 Intergovernmental Panel on Climate Change*. Cambridge University Press, pp. 465–570.
- 824 Collins, H.P., Elliott, E.T., Paustian, K., Bundy, L.G., Dick, W.A., Huggins, D.R., Smucker, A.J.M., Paul, E.A.,
825 2000. Soil carbon pools and fluxes in long-term corn belt agroecosystems. *Soil Biology and
826 Biochemistry* 32, 157–168.
- 827 Crow, S.E., Sierra, C.A., 2018. Dynamic, intermediate soil carbon pools may drive future responsiveness
828 to environmental change. *Journal of environmental quality* 47, 607–616.
- 829 Crowther, T.W., Todd-Brown, K.E., Rowe, C.W., Wieder, W.R., Carey, J.C., Machmuller, M.B., Snoek, B.L.,
830 Fang, S., Zhou, G., Allison, S.D., 2016. Quantifying global soil carbon losses in response to
831 warming. *Nature* 540, 104–108.
- 832 Czimczik, C.I., Masiello, C.A., 2007. Controls on black carbon storage in soils. *Global Biogeochemical
833 Cycles* 21.
- 834 Daly, C., Bryant, K., 2013. *The PRISM climate and weather system—an introduction*. Corvallis, OR: PRISM
835 climate group.

- 836 Dangal, S.R., Sanderman, J., 2020. Is Standardization Necessary for Sharing of a Large Mid-Infrared Soil
837 Spectral Library? *Sensors* 20, 6729.
- 838 Dangal, S.R., Sanderman, J., Wills, S., Ramirez-Lopez, L., 2019. Accurate and precise prediction of soil
839 properties from a large mid-infrared spectral library. *Soil Systems* 3, 11.
- 840 Davidson, E.A., Janssens, I.A., 2006. Temperature sensitivity of soil carbon decomposition and feedbacks
841 to climate change. *Nature* 440, 165–173.
- 842 Del Grosso, S., Ojima, D., Parton, W., Mosier, A., Peterson, G., Schimel, D., 2002. Simulated effects of
843 dryland cropping intensification on soil organic matter and greenhouse gas exchanges using the
844 DAYCENT ecosystem model. *Environmental pollution* 116, S75–S83.
- 845 Del Grosso, S.J., Parton, W.J., Mosier, A.R., Hartman, M.D., Brenner, J., Ojima, D.S., Schimel, D.S., 2001.
846 Simulated interaction of carbon dynamics and nitrogen trace gas fluxes using the DAYCENT
847 model. *Modeling carbon and nitrogen dynamics for soil management* 303–332.
- 848 Deng, L., Zhu, G., Tang, Z., Shangguan, Z., 2016. Global patterns of the effects of land-use changes on soil
849 carbon stocks. *Global Ecology and Conservation* 5, 127–138.
- 850 Doetterl, S., Stevens, A., Six, J., Merckx, R., Van Oost, K., Pinto, M.C., Casanova-Katny, A., Muñoz, C.,
851 Boudin, M., Venegas, E.Z., 2015. Soil carbon storage controlled by interactions between
852 geochemistry and climate. *Nature Geoscience* 8, 780–783.
- 853 Dungait, J.A., Hopkins, D.W., Gregory, A.S., Whitmore, A.P., 2012. Soil organic matter turnover is
854 governed by accessibility not recalcitrance. *Global Change Biology* 18, 1781–1796.
- 855 Eglin, T., Ciais, P., Piao, S.L., Barré, P., Bellassen, V., Cadule, P., Chenu, C., Gasser, T., Koven, C.,
856 Reichstein, M., 2010. Historical and future perspectives of global soil carbon response to climate
857 and land-use changes. *Tellus B: Chemical and Physical Meteorology* 62, 700–718.
- 858 Falcone, J.A., LaMotte, A.E., 2016. National 1-kilometer rasters of selected census of agriculture statistics
859 allocated to land use for the time period 1950 to 2012. US Geological Survey Data Release.
- 860 Fontaine, S., Barot, S., Barré, P., Bdioui, N., Mary, B., Rumpel, C., 2007. Stability of organic carbon in
861 deep soil layers controlled by fresh carbon supply. *Nature* 450, 277–280.
- 862 Gollany, H., 2016. CQESTR simulation of dryland agroecosystem soil organic carbon changes under
863 climate change scenarios. *Synthesis and Modeling of Greenhouse Gas Emissions and Carbon
864 Storage in Agricultural and Forest Systems to Guide Mitigation and Adaptation* 6, 59–87.
- 865 Grandy, A.S., Sinsabaugh, R.L., Neff, J.C., Stursova, M., Zak, D.R., 2008. Nitrogen deposition effects on
866 soil organic matter chemistry are linked to variation in enzymes, ecosystems and size fractions.
867 *Biogeochemistry* 91, 37–49.
- 868 Guo, L.B., Gifford, R.M., 2002. Soil carbon stocks and land use change: a meta analysis. *Global change
869 biology* 8, 345–360.
- 870 Halvorson, A.D., Wienhold, B.J., Black, A.L., 2002. Tillage, nitrogen, and cropping system effects on soil
871 carbon sequestration. *Soil science society of America journal* 66, 906–912.
- 872 Hartman, M.D., Merchant, E.R., Parton, W.J., Gutmann, M.P., Lutz, S.M., Williams, S.A., 2011. Impact of
873 historical land-use changes on greenhouse gas exchange in the US Great Plains, 1883–2003.
874 *Ecological Applications* 21, 1105–1119.
- 875 Hengl, T., Mendes de Jesus, J., Heuvelink, G.B., Ruiperez Gonzalez, M., Kilibarda, M., Blagotić, A.,
876 Shangguan, W., Wright, M.N., Geng, X., Bauer-Marschallinger, B., 2017. SoilGrids250m: Global
877 gridded soil information based on machine learning. *PLoS one* 12, e0169748.
- 878 Hicks, W., Rossel, R.V., Tuomi, S., 2015. Developing the Australian mid-infrared spectroscopic database
879 using data from the Australian Soil Resource Information System. *Soil Research* 53, 922–931.
- 880 Hobbey, E., Baldock, J., Hua, Q., Wilson, B., 2017. Land-use contrasts reveal instability of subsoil organic
881 carbon. *Global Change Biology* 23, 955–965.
- 882 Hsieh, Y.-P., 1993. Radiocarbon signatures of turnover rates in active soil organic carbon pools. *Soil
883 Science Society of America Journal* 57, 1020–1022.

- 884 Ingram, L.J., Stahl, P.D., Schuman, G.E., Buyer, J.S., Vance, G.F., Ganjegunte, G.K., Welker, J.M., Derner,
 885 J.D., 2008. Grazing impacts on soil carbon and microbial communities in a mixed-grass
 886 ecosystem. *Soil Science Society of America Journal* 72, 939–948.
- 887 Jandl, R., Rodeghiero, M., Martinez, C., Cotrufo, M.F., Bampa, F., van Wesemael, B., Harrison, R.B.,
 888 Guerrini, I.A., Richter Jr, D. deB, Rustad, L., 2014. Current status, uncertainty and future needs in
 889 soil organic carbon monitoring. *Science of the total environment* 468, 376–383.
- 890 Janssens, I.A., Dieleman, W., Luysaert, S., Subke, J.-A., Reichstein, M., Ceulemans, R., Ciais, P., Dolman,
 891 A.J., Grace, J., Matteucci, G., 2010. Reduction of forest soil respiration in response to nitrogen
 892 deposition. *Nature geoscience* 3, 315–322.
- 893 Jarvis, A., Reuter, H.I., Nelson, A., Guevara, E., 2008. Hole-filled SRTM for the globe Version 4, available
 894 from the CGIAR-CSI SRTM 90m Database.
- 895 Jobbágy, E.G., Jackson, R.B., 2000. The vertical distribution of soil organic carbon and its relation to
 896 climate and vegetation. *Ecological applications* 10, 423–436.
- 897 Jones, M.B., Donnelly, A., 2004. Carbon sequestration in temperate grassland ecosystems and the
 898 influence of management, climate and elevated CO₂. *New Phytologist* 164, 423–439.
- 899 Kelly, R.H., Parton, W.J., Hartman, M.D., Stretch, L.K., Ojima, D.S., Schimel, D.S., 2000. Intra-annual and
 900 interannual variability of ecosystem processes in shortgrass steppe. *Journal of Geophysical*
 901 *Research: Atmospheres* 105, 20093–20100.
- 902 Kittel, T.G., Rosenbloom, N.A., Royle, J.A., Daly, C., Gibson, W.P., Fisher, H.H., Thornton, P., Yates, D.N.,
 903 Aulenbach, S., Kaufman, C., 2004. VEMAP phase 2 bioclimatic database. I. Gridded historical
 904 (20th century) climate for modeling ecosystem dynamics across the conterminous USA. *Climate*
 905 *Research* 27, 151–170.
- 906 Klein Goldewijk, K., Beusen, A., Doelman, J., Stehfest, E., 2017. Anthropogenic land use estimates for the
 907 Holocene–HYDE 3.2. *Earth System Science Data* 9, 927–953.
- 908 Knorr, W., Prentice, I.C., House, J.I., Holland, E.A., 2005. Long-term sensitivity of soil carbon turnover to
 909 warming. *Nature* 433, 298–301.
- 910 Lal, R., 2018. Digging deeper: A holistic perspective of factors affecting soil organic carbon sequestration
 911 in agroecosystems. *Global Change Biology* 24, 3285–3301.
- 912 Lal, R., 2004. Carbon sequestration in dryland ecosystems. *Environmental management* 33, 528–544.
- 913 Lavalley, J.M., Soong, J.L., Cotrufo, M.F., 2020. Conceptualizing soil organic matter into particulate and
 914 mineral-associated forms to address global change in the 21st century. *Global Change Biology*
 915 26, 261–273.
- 916 Lee, J., Viscarra Rossel, R.A., 2020. Soil carbon simulation confounded by different pool initialisation.
 917 *Nutrient Cycling in Agroecosystems* 116, 245–255.
- 918 Liebig, M.A., Gross, J.R., Kronberg, S.L., Phillips, R.L., 2010. Grazing management contributions to net
 919 global warming potential: A long-term evaluation in the Northern Great Plains. *Journal of*
 920 *Environmental Quality* 39, 799–809.
- 921 Luo, Y., Ahlström, A., Allison, S.D., Batjes, N.H., Brovkin, V., Carvalhais, N., Chappell, A., Ciais, P.,
 922 Davidson, E.A., Finzi, A., 2016. Toward more realistic projections of soil carbon dynamics by
 923 Earth system models. *Global Biogeochemical Cycles* 30, 40–56.
- 924 Luo, Z., Feng, W., Luo, Y., Baldock, J., Wang, E., 2017. Soil organic carbon dynamics jointly controlled by
 925 climate, carbon inputs, soil properties and soil carbon fractions. *Global Change Biology* 23,
 926 4430–4439.
- 927 Metherell, A., Harding, L., Cole, C., Parton, W., 1994. CENTURY soil organic matter model environment,
 928 technical documentation, agroecosystem version 4.0 GPSR Technical Report No. 4. Great Plains
 929 System Research Unit, USDA-ARS, Fort Collins, CO.
- 930 Nachtergaele, F., van Velthuisen, H., Verelst, L., 2012. Harmonized World Soil Database Version 1.2.
 931 Food and Agriculture Organization of the United Nations (FAO). International Institute for

- 932 Applied Systems Analysis (IIASA), ISRIC-World Soil Information, Institute of Soil Science–Chinese
 933 Academy of Sciences (ISSCAS), Joint Research Centre of the European Commission (JRC).
- 934 Ogle, S.M., Breidt, F.J., Easter, M., Williams, S., Killian, K., Paustian, K., 2010. Scale and uncertainty in
 935 modeled soil organic carbon stock changes for US croplands using a process-based model.
 936 *Global Change Biology* 16, 810–822.
- 937 Omernik, J.M., Griffith, G.E., 2014. Ecoregions of the conterminous United States: evolution of a
 938 hierarchical spatial framework. *Environmental management* 54, 1249–1266.
- 939 Page, K.L., Dalal, R.C., Dang, Y.P., 2014. How useful are MIR predictions of total, particulate, humus, and
 940 resistant organic carbon for examining changes in soil carbon stocks in response to different
 941 crop management? A case study. *Soil Research* 51, 719–725.
- 942 Parton, W.J., Hartman, M., Ojima, D., Schimel, D., 1998. DAYCENT and its land surface submodel:
 943 description and testing. *Global and planetary Change* 19, 35–48.
- 944 Parton, W.J., Schimel, D.S., Cole, C.V., Ojima, D.S., 1987. Analysis of factors controlling soil organic
 945 matter levels in Great Plains grasslands. *Soil Science Society of America Journal* 51, 1173–1179.
- 946 Parton, W.J., Stewart, J.W., Cole, C.V., 1988. Dynamics of C, N, P and S in grassland soils: a model.
 947 *Biogeochemistry* 5, 109–131.
- 948 Paul, E.A., Morris, S.J., Bohm, S., 2001. The determination of soil C pool sizes and turnover rates:
 949 biophysical fractionation and tracers. *Assessment methods for soil carbon* 14, 193–206.
- 950 Poeplau, C., Don, A., 2013. Sensitivity of soil organic carbon stocks and fractions to different land-use
 951 changes across Europe. *Geoderma* 192, 189–201.
- 952 Ramcharan, A., Hengl, T., Nauman, T., Brungard, C., Waltman, S., Wills, S., Thompson, J., 2018. Soil
 953 property and class maps of the conterminous United States at 100-meter spatial resolution. *Soil
 954 Science Society of America Journal* 82, 186–201.
- 955 Ramirez-Lopez, L., Behrens, T., Schmidt, K., Stevens, A., Demattê, J.A.M., Scholten, T., 2013. The
 956 spectrum-based learner: A new local approach for modeling soil vis–NIR spectra of complex
 957 datasets. *Geoderma* 195, 268–279.
- 958 Rasmussen, C., Heckman, K., Wieder, W.R., Keiluweit, M., Lawrence, C.R., Berhe, A.A., Blankinship, J.C.,
 959 Crow, S.E., Druhan, J.L., Pries, C.E.H., 2018. Beyond clay: towards an improved set of variables
 960 for predicting soil organic matter content. *Biogeochemistry* 137, 297–306.
- 961 Riahi, K., Rao, S., Krey, V., Cho, C., Chirkov, V., Fischer, G., Kindermann, G., Nakicenovic, N., Rafaj, P.,
 962 2011. RCP 8.5—A scenario of comparatively high greenhouse gas emissions. *Climatic change*
 963 109, 33–57.
- 964 Sanderman, J., Baldock, J.A., Dangal, S.R., Ludwig, S., Potter, S., Rivard, C., Savage, K., 2021. Soil organic
 965 carbon fractions in the Great Plains of the United States: an application of mid-infrared
 966 spectroscopy. *Biogeochemistry* 1–18.
- 967 Sanderman, J., Creamer, C., Baisden, W.T., Farrell, M., Fallon, S., 2017a. Greater soil carbon stocks and
 968 faster turnover rates with increasing agricultural productivity. *Soil* 3, 1–16.
- 969 Sanderman, J., Hengl, T., Fiske, G.J., 2017b. Soil carbon debt of 12,000 years of human land use.
 970 *Proceedings of the National Academy of Sciences* 114, 9575–9580.
- 971 Sanford Jr, R.L., Parton, W.J., Ojima, D.S., Lodge, D.J., 1991. Hurricane effects on soil organic matter
 972 dynamics and forest production in the Luquillo Experimental Forest, Puerto Rico: results of
 973 simulation modeling. *Biotropica* 364–372.
- 974 Schmer, M.R., Jin, V.L., Wienhold, B.J., Varvel, G.E., Follett, R.F., 2014. Tillage and residue management
 975 effects on soil carbon and nitrogen under irrigated continuous corn. *Soil Science Society of
 976 America Journal* 78, 1987–1996.
- 977 Schmidt, M.W., Torn, M.S., Abiven, S., Dittmar, T., Guggenberger, G., Janssens, I.A., Kleber, M., Kögel-
 978 Knabner, I., Lehmann, J., Manning, D.A., 2011. Persistence of soil organic matter as an
 979 ecosystem property. *Nature* 478, 49–56.

- 980 Schwalm, C.R., Glendon, S., Duffy, P.B., 2020. RCP8. 5 tracks cumulative CO₂ emissions. Proceedings of
 981 the National Academy of Sciences 117, 19656–19657.
- 982 Sherrod, L.A., Peterson, G.A., Westfall, D.G., Ahuja, L.R., 2005. Soil organic carbon pools after 12 years in
 983 no-till dryland agroecosystems. Soil Science Society of America Journal 69, 1600–1608.
- 984 Shi, Z., Crowell, S., Luo, Y., Moore, B., 2018. Model structures amplify uncertainty in predicted soil
 985 carbon responses to climate change. Nature communications 9, 1–11.
- 986 Sindelar, A.J., Schmer, M.R., Jin, V.L., Wienhold, B.J., Varvel, G.E., 2015. Long-term corn and soybean
 987 response to crop rotation and tillage. Agronomy Journal 107, 2241–2252.
- 988 Sinsabaugh, R.L., Gallo, M.E., Lauber, C., Waldrop, M.P., Zak, D.R., 2005. Extracellular enzyme activities
 989 and soil organic matter dynamics for northern hardwood forests receiving simulated nitrogen
 990 deposition. Biogeochemistry 75, 201–215.
- 991 Six, J., Conant, R.T., Paul, E.A., Paustian, K., 2002. Stabilization mechanisms of soil organic matter:
 992 implications for C-saturation of soils. Plant and soil 241, 155–176.
- 993 Skjemstad, J.O., Spouncer, L.R., Cowie, B., Swift, R.S., 2004. Calibration of the Rothamsted organic
 994 carbon turnover model (RothC ver. 26.3), using measurable soil organic carbon pools. Soil
 995 Research 42, 79–88.
- 996 Sohl, T.L., Sleeter, B.M., Sayler, K.L., Bouchard, M.A., Reker, R.R., Bennett, S.L., Sleeter, R.R., Kanengieter,
 997 R.L., Zhu, Z., 2012. Spatially explicit land-use and land-cover scenarios for the Great Plains of the
 998 United States. Agriculture, Ecosystems & Environment 153, 1–15.
- 999 Stockmann, U., Adams, M.A., Crawford, J.W., Field, D.J., Henakaarchchi, N., Jenkins, M., Minasny, B.,
 1000 McBratney, A.B., De Courcelles, V. de R., Singh, K., 2013. The knowns, known unknowns and
 1001 unknowns of sequestration of soil organic carbon. Agriculture, Ecosystems & Environment 164,
 1002 80–99.
- 1003 Sulman, B.N., Moore, J.A., Abramoff, R., Averill, C., Kivlin, S., Georgiou, K., Sridhar, B., Hartman, M.D.,
 1004 Wang, G., Wieder, W.R., 2018. Multiple models and experiments underscore large uncertainty in
 1005 soil carbon dynamics. Biogeochemistry 141, 109–123.
- 1006 Syswerda, S.P., Corbin, A.T., Mokma, D.L., Kravchenko, A.N., Robertson, G.P., 2011. Agricultural
 1007 management and soil carbon storage in surface vs. deep layers. Soil Science Society of America
 1008 Journal 75, 92–101.
- 1009 Tangen, B.A., Bansal, S., 2020. Soil organic carbon stocks and sequestration rates of inland, freshwater
 1010 wetlands: Sources of variability and uncertainty. Science of The Total Environment 749, 141444.
- 1011 Thomson, A.M., Calvin, K.V., Smith, S.J., Kyle, G.P., Volke, A., Patel, P., Delgado-Arias, S., Bond-Lamberty,
 1012 B., Wise, M.A., Clarke, L.E., 2011. RCP4. 5: a pathway for stabilization of radiative forcing by
 1013 2100. Climatic change 109, 77–94.
- 1014 Thornton, P.E., Thornton, M.M., Mayer, B.W., Wilhelmi, N., Wei, Y., Devarakonda, R., Cook, R., 2012.
 1015 Daymet: Daily surface weather on a 1 km grid for North America, 1980-2008. Oak Ridge National
 1016 Laboratory (ORNL) Distributed Active Archive Center for Biogeochemical Dynamics (DAAC).
- 1017 Tian, H., Lu, C., Yang, J., Banger, K., Huntzinger, D.N., Schwalm, C.R., Michalak, A.M., Cook, R., Ciais, P.,
 1018 Hayes, D., 2015. Global patterns and controls of soil organic carbon dynamics as simulated by
 1019 multiple terrestrial biosphere models: Current status and future directions. Global
 1020 Biogeochemical Cycles 29, 775–792.
- 1021 Todd-Brown, K.E.O., Randerson, J.T., Hopkins, F., Arora, V., Hajima, T., Jones, C., Shevliakova, E., Tjiputra,
 1022 J., Volodin, E., Wu, T., 2014. Changes in soil organic carbon storage predicted by Earth system
 1023 models during the 21st century. Biogeosciences 11, 2341–2356.
- 1024 Torn, M.S., Kleber, M., Zavaleta, E.S., Zhu, B., Field, C.B., Trumbore, S.E., 2013. A dual isotope approach
 1025 to isolate soil carbon pools of different turnover times. Biogeosciences 10, 8067–8081.
- 1026 Torn, M.S., Trumbore, S.E., Chadwick, O.A., Vitousek, P.M., Hendricks, D.M., 1997. Mineral control of soil
 1027 organic carbon storage and turnover. Nature 389, 170–173.

- 1028 Trumbore, S.E., 1997. Potential responses of soil organic carbon to global environmental change.
1029 Proceedings of the National Academy of Sciences 94, 8284–8291.
- 1030 Van Groenigen, K.J., Qi, X., Osenberg, C.W., Luo, Y., Hungate, B.A., 2014. Faster decomposition under
1031 increased atmospheric CO₂ limits soil carbon storage. *Science* 344, 508–509.
- 1032 Wieder, W.R., Hartman, M.D., Sulman, B.N., Wang, Y.-P., Koven, C.D., Bonan, G.B., 2018. Carbon cycle
1033 confidence and uncertainty: Exploring variation among soil biogeochemical models. *Global
1034 change biology* 24, 1563–1579.
- 1035 Wiesmeier, M., Urbanski, L., Hobbey, E., Lang, B., von Lützow, M., Marin-Spiotta, E., van Wesemael, B.,
1036 Rabot, E., Ließ, M., Garcia-Franco, N., 2019. Soil organic carbon storage as a key function of soils-
1037 A review of drivers and indicators at various scales. *Geoderma* 333, 149–162.
- 1038 Zimmermann, M., Leifeld, J., Schmidt, M.W.I., Smith, P., Fuhrer, J., 2007. Measured soil organic matter
1039 fractions can be related to pools in the RothC model. *European Journal of Soil Science* 58, 658–
1040 667.
- 1041
- 1042